Fusion Engineering and Design 174 (2022) 112966

Contents lists available at ScienceDirect

Fusion Engineering and Design

journal homepage: www.elsevier.com/locate/fusengdes

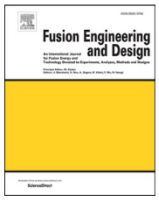

Containment structures and port configurations

C. Bachmann [a,b,*], L. Ciupinski [c], C. Gliss [a], T. Franke [a,d], T. Härtl [d], P. Marek [e], F. Maviglia [a,f], R. Mozzillo [g], R. Pielmeier [h], T. Schiller [h], P. Spaeh [j], T. Steinbacher [a], M. Stetka [h], T. Todd [i], C. Vorpahl [j]

[a] EUROfusion Consortium, Garching, Boltzmannstr. 2, Germany
[b] Technical University of Denmark, Lyngby, Denmark
[c] Faculty of Materials Science and Engineering, Warsaw University of Technology, Woloska 141, 02-507, Warsaw, Poland
[d] Max Planck Institute for Plasma Physics, Garching, Germany
[e] Faculty of Power and Aeronautical Engineering, Warsaw University of Technology, Nowowiejska 24, 00-665, Warsaw, Poland
[f] Associazione EURATOM-ENEA sulla Fusione, C.R. Frascati, C.P. 65-00044 Frascati, Rome, Italy
[g] CREATE, Engineering School of Basilicata University, Campus Macchia Romana (PZ), 85100, Italy
[h] MAN Energy Solutions SE, Werftstraße 17, 94469 Deggendorf, Germany
[i] UKAEA, Culham Science Centre, Abingdon, Oxon, OX14 3DB, UK (retired)
[j] Karlsruhe Institute of Technology (KIT), 76344 Eggenstein-Leopoldshafen, Germany

ARTICLE INFO

Keywords:
DEMO
Tokamak
Vacuum vessel
Cryostat
In-vessel components
Breeding blanket
Design integration

ABSTRACT

This article describes the DEMO cryostat, the vacuum vessel, and the tokamak building as well as the system configurations to integrate the main in-vessel components and auxiliary systems developed during the Pre-Conceptual Design Phase.

The vacuum vessel is the primary component for radiation shielding and containment of tritium and other radioactive material. Various systems required to operate the plasma are integrated in its ports. The vessel together with the external magnetic coils is located inside the even larger cryostat that has the primary function to provide a vacuum to enable the operation of the superconducting coils in cryogenic condition. The cryostat is surrounded by a thick concrete structure: the bioshield. It protects the external areas from neutron and gamma radiation emitted from the tokamak. The tokamak building layout is aligned with the VV ports implementing floors and separate rooms, so-called port cells, that can be sealed to provide a secondary confinement when a port is opened during in-vessel maintenance.

The ports of the torus-shaped VV have to allow for the replacement of in-vessel components but also incorporate plasma limiters and auxiliary heating and diagnostic systems. The divertor is replaced through horizontal ports at the lower level, the breeding blanket (BB) through upper vertical ports. The pipe work of these in-vessel components is also routed through these ports. To facilitate the vertical replacement of the BB, it is divided into large vertical segments. Their mechanical support during operation relies on vertically clamping them inside the vacuum vessel by a combination of obstructed thermal expansion and radial pre-compression due to the ferromagnetic force acting on the breeding blanket structural material in the toroidal magnetic field.

1. Introduction

The EU fusion roadmap [1] foresees the development of the Demonstration Fusion Power Plant (DEMO) in Europe to follow ITER. The first DEMO development phase, the Pre-Conceptual Design (PCD) Phase, has recently been concluded proposing a tokamak machine around a plasma with a major radius of ~9 m and a fusion power of ~2000 MW [2]. The inter-dependency of the design of one system on the requirements of other systems had early been recognized. The PCD Phase had consequently been focused on an integrated design approach to define a tokamak and plant configuration suitable to meet the main goals of DEMO [3]: (i) production of few hundred MWs of net electricity, (ii) tritium self-sufficiency, (iii) adequate availability, (iv) minimization of activation waste, and (v) testing of key technologies for future fusion power plants [2].

The basic design of the containment structures, i.e. vacuum vessel (VV), cryostat and tokamak building, must enable the integration of the various tokamak and plant systems and at the same time ensure the

* Corresponding author.

https://doi.org/10.1016/j.fusengdes.2021.112966
Received 2 August 2021; Received in revised form 29 November 2021; Accepted 29 November 2021
Available online 14 December 2021
0920-3796/© 2021 The Author(s). Published by Elsevier B.V. This is an open access article under the CC BY license (http://creativecommons.org/licenses/by/4.0/).

safety of the plant.

The cryostat, see Section 2, is a large vacuum chamber that contains and mechanically supports the tokamak. It has large openings that correspond to the VV ports. These are connected to the cryostat by large metallic bellows.

The VV, see Section 3, is fundamental to the design of the tokamak. It affects the electromagnetic (EM) control of the plasma and is also the support structure that allows the installation and precise alignment of the in-vessel components (IVCs), [12]. It must withstand extremely large EM loads. The configuration of the VV ports, i.e. their location and size in-between the magnetic coils, must be suitable to permit the installation of various auxiliary systems required to operate and control the plasma and also to enable the replacement of the IVCs.

The tokamak building, see Section 4, includes outside the cryostat the cylindrical ~2 m thick bioshield made of concrete that protects the building areas from neutron and gamma radiation. The external walls of the tokamak building are the ultimate boundary to the environment for radiation hazards.

In the early design phase of DEMO the approach taken in ITER has been adopted where the VV provides primary and the building structure provides secondary confinement [4]. However, it is planned to investigate also an alternative in the future, i.e. to transfer the function to confine the radioactive material inside the VV from the VV to the cryostat. While the VV would then be relieved from stringent quality assurance requirements such as regular in-service inspections, the cryostat would need to be constructed following the rigorous rules defined in design codes such as those for fission reactor pressure vessels, e.g. RCC-MR.

The configuration of the IVCs incl. the port plugs was defined such that the DEMO goals can be reached but also aiming at their relevance for future fusion power plants:

- The impact areas on the plasma-facing wall of charged particles are controlled and limited. Plasma limiters are installed in discrete locations and protect the wall of the breeding blanket (BB) and of the heating and diagnostic systems [5]. The divertor targets, which are subject to very high particle loads and susceptible to failure are mounted to cassettes that can be well accessed and replaced through the lower ports, see section 5.
- The BB is divided into large vertical segments that can be removed through the large upper ports in a reasonably short plant downtime, see Section 6. Their mechanical supports were devised minimizing the remote handling (RH) operations required for their engagement and release, see Section 8. Thus it was possible to avoid operating RH tools in front of the highly activated plasma-facing components for BB replacement [6, 8].
- The auxiliary systems are predominantly installed in the equatorial ports with minimum obstruction to the port closure plate and good access to the fixations of the port plug, see section 7.

Two concepts of the BB were pursued in the PCD Phase, the water-cooled lithium lead (WCLL) and the helium-cooled pebble bed (HCPB). However, the design and configuration of all other tokamak components with exception of the BB service pipes is independent of the BB concept.

2. Cryostat

2.1. Main functions and configuration

The cryostat provides a vacuum environment to avoid heat transfer by gas conduction and convection to the superconducting coils and the thermal shields. To withstand the external pressure it is cylindrical and has a top lid roughly shaped like a torispherical head, see Fig. 2. As it is not actively cooled or heated its temperature is close to ambient. A massive ring structure, the pedestal ring, is integrated in the lower part of the cryostat and supports the tokamak, providing a safety-important function. These parts of the cryostat are therefore designed in accordance with nuclear codes while the majority of the cryostat is designed as a conventional vacuum vessel.

Large openings provide access for maintenance inside the cryostat and to the VV ports. The port ducts are connected to the cryostat by large metallic bellows to compensate relative displacements and to segregate the port cells from each other, see Section 4. In addition several penetrations are integrated into the cryostat for the magnet feeders, the cooling pipes for VV and thermal shields, the cryostat vacuum pumps, and in-cryostat diagnostic systems. Large leaks of cryogenic helium have the potential to cause an internal over-pressurization, which is intended to be limited to 1.5 bar either by a suitable layout of the cryogenic system or by the implementation of a cryostat venting and overpressure protection system, e.g. remotely operated vacuum valves. The cryostat cylinder may therefore require supports against lifting forces.

2.2. Design concept

The cryostat concept described here is an ITER-like self-supported vacuum chamber [9, 10] that also transfers the tokamak weight vertically into the concrete crown on the building basemat and – in case of a seismic event – horizontally to the bioshield. A different, non-self-supported concept of the cryostat was also developed and is described in [11]. There, the bioshield supports the cryostat main cylinder and top lid. This would allow a substantial reduction of the amount of steel in these components. However, in case the first confinement function was assigned to the cryostat, the bioshield and the bioshield roof would also need to be classified as safety-important class 1 (SIC-1) components. The consequent cost increase might outweigh the cost saving achieved with the lighter non-self-supported cryostat.

2.3. Design

The cryostat base section is a cylindrical extension below the pedestal ring with reduced diameter. It allows the integration of the magnet feeders. For the bottom lid a flat double-wall structure rather than a dome-shape has been chosen to reduce the vertical space requirement. The pedestal ring has a rectangular cross-section of ~1.5 $m \times 1.5$ m. Its lower plate is the pressure boundary and so the tokamak support structures will be fixed to the upper plate using bolts and nuts. The skirt with a thickness of 100 mm extends the pedestal ring radially to transfer sideways loads acting on the tokamak to the bioshield. For this purpose large shear keys are welded to the skirt that are engaged in corresponding recesses in the bioshield to transfer toroidal or lateral forces, see ITER cryostat design [9].

The main cylinder is a welded structure made of 55 mm thick steel plates that are reinforced by T-stiffeners to avoid buckling. Large cut-outs in the main cylinder allow access to the VV ports, which are connected to the cryostat by metallic bellows. The main cylinder rests on a radial extension of the bioshield on vertical supports that are equally distributed along the circumference supporting the weight of the main cylinder and the top lid as well as the pressure acting on the top lid, see Fig. 2.

The top lid consists of a dome-shaped shell supported by 16 radial girders that are joined in the center to two large ring structures. Large trapezoidal openings allow access to the VV upper ports but at the same time considerably reduce the membrane stiffness of the dome. The two massive ring structures, each with a cross-section of ~0.2m^2, effectively oppose radial contraction and hence enable the girders to reduce the vertical deflection of the top lid due to the external pressure. The shallow dome shape with reinforcing girders was chosen as it matches the available space between the bioshield roof (see Section 4) and the VV upper ports, see Fig. 8. The compact design of the upper part of the tokamak reduces the distance between the bioshield roof and the tokamak machine and facilitates the upper port maintenance.

3. Vacuum vessel

3.1. Functions and basic design

The VV is a double-shell welded structure made of austenitic steels 316L(N)-IG and XM-19. Each of its sectors integrate one lower horizontal port (Section 5), one upper vertical port (Section 6), and one equatorial port (Section 7). Within most of these ports removable port plugs are integrated via bolted flanges. In the inner shell of the VV the support structures for the IVCs are implemented (Section 8), see Fig. 4. Table 1.

The VV enables the ultra-high vacuum conditions required to operate the plasma ($<10^{-5}$ Pa). In DEMO, the main function of the blanket is to breed tritium rather than to shield neutrons. In fact, the BB reduces the neutron flux by approximately one order of magnitude only [7]. In order to provide adequate neutron shielding to the superconducting coils the VV further reduces the neutron flux by approximately 5 orders of magnitude [8]. For this purpose steel plates are stacked into the interspace of the double-wall structure, see Fig. 3. The heat generated in the VV during plasma operation by the absorption of neutrons is removed by an active cooling water loop. In case of severe accidents this also serves as the decay heat removal system. Table 2 provides an overview of the main VV parameters as defined in the DEMO PCD Phase.

Being a toroidally continuous conductive structure in proximity of the plasma the VV provides a degree of passive stability to the plasma. Since the toroidal continuity is interrupted by the VV ports the inner shell above and below the equatorial ports is particularly important in this respect.

The VV functions as the first confinement barrier for the activated dust and tritium inside. For this reason and for the relative pressure being >0.5 bar it is subject to nuclear regulation and designed as nuclear pressure equipment.

A more comprehensive summary of the functions of the VV is provided in [12].

3.2. Material selection

As in ITER [14, 15] and other fusion devices e.g. K-STAR [16] and W-7X [17], austenitic steels were chosen for the structural parts of the VV for their good mechanical properties and good weldability. The degradation of their mechanical properties due to the high neutron fluence in DEMO remains negligible up to at least 2.75 dpa [8, 18].

At the same time it is recognized that the high nickel content of austenitic steels leads to the generation of long-lived isotopes, in particular in the inner shell and parts of the ribs. Considering today's waste classification criteria these parts will require storage in intermediate level waste depositories for several hundred years. This makes the VV a major contributor to the overall DEMO activation waste [19]. Consequently, efforts were made to reduce the amount of activation waste stemming from the VV: (i) the inner shell thickness was reduced from 60 mm to 32/36 mm (inboard/outboard) and (ii) EUROFER [20] instead of austenitic steel is used for those in-wall shielding plates behind the inner shell that are subject to high neutron fluence, see Fig. 3.

The drive to improve the waste prospects of the DEMO VV has led to further consideration of the use of non-austenitic steels. It was concluded however that the irradiation resistance of ferritic steels (~0.1 dpa [21]) is insufficient. Ferritic-martensitic steels such as EUROFER have poor machining, poor forming and poor welding characteristics. Particularly the need for post-weld heat treatments at 760–800 °C makes EUROFER unsuitable for the fabrication of a complex and large DEMO VV sector and especially for the assembly welds in the tokamak pit.

Table 1
Cryostat parameters.

Pressure (abs.) inside/outside OperationAccident	10^{-4} Pa / 1 bar <1.5 bar / 1 bar
Temperature	20–30 °C
Material	316L(N)
Mass Diameter Height Free volume	~6000 tons ~40 m ~36 m ~27,000 m^3
Plate thicknesses Main cylinder Top lid Skirt Pedestal ring	55 mm 70 mm 100 mm 200 mm

Table 2
Vacuum vessel parameters.

Design pressure (abs.), Cat. III/IV	1.5 / 2.0 bar
Coolant pressure plasma operation baking	11 bar 21 bar
Operating temperature [13] plasma operation (inlet/outlet) baking	40/60 °C 180 °C
Heat generation (WCLL / HCPB) plasma operation 1 month after shutdown	8/45 MW 0.6 / 4 kW
Material (inner/outer shell, ribs) inboard outboard	XM-19 316L(N)-IG
Plate thicknesses inboard (inner/outer shell) outboard ribs (inboard/outboard) ribs behind BB supports	32/42 mm 36 mm 25/30 mm 60 mm

3.3. Design and fabrication

The following aspects were considered in the development of the DEMO VV design: Small shape tolerances, fabrication and qualification, assembly, in-service inspection, loads, neutron shielding and cost:

The VV is toroidally divided into sectors, each corresponding to one toroidal field (TF) coil. Consequently, the VV ports are located on the sector field joints where the sectors are joined during tokamak assembly by welded splice plates that compensate tolerances. Into the double-wall structure of each sector the port stubs are implemented. After assembly of the VV sectors with the TF coils the ports are welded to the port stubs in the tokamak pit, see Fig. 4. Should an assembly crane with greater load capacity be available, larger VV sectors should be considered to reduce the number splice plates, e.g. as in ITER corresponding to two TF coils.

No plates with double-curvature or 3D-formed parts are foreseen. Instead the VV is toroidally segmented, the inner shell based on the BB segments, the outer shell based on the TF coils. Bending moments arising on the inboard wall can be sustained as the toroidal ribs resist shearing forces between the two shells.

The VV must be manufactured to very tight tolerances requirements to allow precise installation of the IVCs and port plugs. In order to reduce weld shrinkage narrow-gap TIG is foreseen as the primary welding technology. In addition, each VV sector is foreseen to be manufactured in the following sequence: First the entire inner shell, second the ribs, third the outer shell and last the port stubs. The continuous control of the shape deviations throughout this process is expected to allow to some degree their correction in subsequent fabrication steps, ultimately achieving shape tolerances of approximately ±20–30 mm. As a drawback the industrial capability for parallel manufacturing of such large VV sectors can be expected to be limited also at a future time when DEMO might be constructed.

In-service inspection of the VV welds, as required by relevant nuclear design codes, is a considerable challenge not only due to the residual gamma radiation but in particular due to the poor accessibility of the VV shells. The presence of the IVCs means that access to the inner shell from inside the VV is possible only during their replacement. A few tens of centimeters of space between the VV outer shell and the VV thermal shield could be provided on the outboard side. On the inboard side however, the cost of space is prohibitive since the tokamak is built as compactly as possible to allow the operation of the plasma in as high a toroidal field as possible [22]. Consequently, welds in the inner and outer shells on the inboard wall are avoided as far as possible making them of single large sheets. Therefore, residual stresses after fabrication and assembly due to the welding process are reduced or even avoided in these large sections of the VV shells. Hence in the first load cycle, the stresses generated will be in the elastic range of the material that will

therefore not undergo plastic deformation, which would affect the alignment of the plasma-facing wall.

The inboard wall is the highest loaded part of the DEMO VV. Large radial pressure occurs due to the ferromagnetic force acting on the IVCs and in addition during a fast discharge of the TF coils (TFCFD) due to induced poloidal currents [6]. In fact, the time constant of the fast discharge should be larger than ~15 s to avoid unsustainable EM loads in the VV. The high strength steel XM-19 is used for strengthening the inboard wall, which allowed reducing the thickness of the VV shells. Secondly, toroidal rather than poloidal ribs are incorporated between the two shells. Both measures do not reduce the electrical resistivity in poloidal direction and therefore do not increase the EM loads during a TFCFD.

To provide good accessibility to the assembly welds on the outer shell splice plates the inner shell splice plate on the inboard has a width of 500 mm (see Fig. 4). After the outer shell splice plate has been welded during assembly the toroidal ribs in the inboard field joint area are welded to the outer shell and the poloidal gussets. The inner shell splice plate will be welded as in ITER to the inner shell only.

3.4. Verification

Primarily two loads drive the design of the VV: (i) the required thickness of the shells is defined by the radial pressure on the inboard wall that is most significant during a TFCFD, and (ii) the spacing of the ribs is defined by the coolant pressure during baking. The VV design has been verified against these load conditions using a finite element model of one sector. Elastoplastic analyses were carried out according to the criteria defined in RCC-MR. Considering dead weight, coolant pressure, interface loads on the IVCs supports and the loads due to a TFCFD with only 15 s discharge time constant it was found that the VV inboard wall meets the criteria (with a small margin of 8%), which demonstrates in general the adequate load bearing capacity of this early design concept. The high elastic membrane stresses that occur in this load case are shown in Fig. 5.

The large net loads that occur during downward vertical displacement events (VDEs) are of lower significance as compared to ITER where the vertical reaction forces on the VV supports can increase by more than a factor of 2 due to VDEs [23]. VDE loads are less significant to the design of the DEMO VV since the dead weight is much larger due to the high mass of the BB, in particular if lead is used as the neutron multiplier. The vertical loads on the DEMO VV supports are assessed in [24] and the lower ports were found suitable to support the VV.

It is expected that local reinforcements will be required at some of the IVC supports and where the port stubs are integrated into the main VV body.

4. Tokamak complex building

4.1. Overview

The DEMO tokamak complex currently consists of three buildings: the tokamak building, the tritium building and the diagnostic building, see Fig. 6. It is a large reinforced concrete structure with dimensions of approx. 141 $m \times 98\ m \times 90$ m and is described in [25]. The complex shares a common rectangular basemat to minimize relative vertical displacements and to install seismic isolators between the ground and the building as in ITER [27]. As the DEMO site has not yet been selected the seismic spectrum of the ITER Cadarache site is used as the design basis [26]. The seismic isolators reduce significantly the seismic loads to be considered in the design of the systems and components inside the tokamak complex. The floor of the heating neutral beam (HNB) cell was defined at ground level to simplify the installation of the heavy HNB vessel without a lifting operation and to limit the height of the assembly hall.

The tokamak complex is the second and ultimate boundary to the environment for radiation hazards. Also the diagnostic building is defined as a confinement barrier to avoid the classification of the numerous penetrations between the two buildings as confinement penetrations.

4.2. Tokamak building

The tokamak building houses the tokamak and numerous plant systems. It is designed to permit assembly and operation of the DEMO tokamak with 16 sectors, each with radial ports at three building floor levels and one vertical upper port. The general architectural structure is arranged around the tokamak implementing a cylindrical bioshield with 2 m wall thickness around the cryostat.

The general arrangement of the building follows the levels of the machine ports, see Fig. 7. The upper and lower pipe chases are arranged with the upper and lower port annexes. Two levels are defined with the lower and equatorial ports. The vertical upper port connects the machine to the maintenance hall to allow for the blanket replacement. There are also two intermediate levels in the tokamak building, the upper feeder and the Q-level. They have no access to the tokamak machine via VV ports and are therefore better protected from neutron and gamma radiation. These levels are dedicated to magnet & thermal shield feeders and allow the installation of cubicles or other radiation sensitive equipment. The concrete dome above the maintenance hall is resistant to a potential airplane crash. It is also the ultimate confinement barrier and provides radiation shielding to the environment during in-vessel maintenance from the top → skyshine [28].

In-vessel maintenance through any VV port is carried out from within a sealed port cell the volume of which is under tritium control, see Fig. 6.

Three types of vertical shafts are implemented inside the tokamak building with dedicated purposes:

- The activated cooling water of the divertor & limiter cooling systems containing ^{16}N, ^{17}N isotopes is vertically routed between the cryostat and the 2 m thick bioshield making use of its shielding function.
- Port cell vertical shafts containing pipework running from the lower to the upper pipe chase serving the port cell on the different levels.
- Gallery vertical shafts in the peripheral areas of the building used to route cable traces and building services and a dedicated HVAC shaft.

The roof of the bioshield is also the floor of the upper maintenance hall. It comprises a steel structure and concrete inserts that can be individually removed to provide access to the VV upper ports and into the cryostat for maintenance including the removal of the central solenoid, see Fig. 8. In the non-nuclear phase the bioshield roof can also be removed entirely by the overhead crane to access the tokamak for major repair works.

5. Lower ports

5.1. Overview

The lower ports fulfill five main functions:

i Provide access for divertor maintenance,
ii Integrate the pipe work of the divertor and, if required, of the BB,
iii Given the higher pressure of exhaust gasses below the divertor the torus vacuum pumps are hosted in some of the lower ports.
iv The VV is supported via the lower ports on the cryostat pedestal ring.
v Provide adequate neutron and radiation shielding to protect the superconducting coils and to permit man-access into the cryostat.

It has not yet been decided whether all lower ports will be used to replace the divertor or if instead some will be dedicated to RH for that purpose and the vacuum pumps will be semi-permanently installed in

the remaining ports. Hence three types of lower port configurations are currently considered, see Table 3.

5.2. Configuration

The lower port size and shape are strongly driven by space constraints and technical requirements [25]. The necessary internal dimension of the port towards the vessel is defined by (i) the need to access the back surface of the IVCs to integrate the feeding pipes, (ii) the size of the divertor cassettes and their extraction kinematics considering also the necessary remote maintenance devices, which operate inside the port, (iii) the size of the torus vacuum pump unit considering also its RH scheme as well as the required free pumping path to the area behind the divertor.

The space available for the lower ports is also constrained by the magnetic coils. In addition, to increase the volume of the outboard BB segment and hence its tritium breeding performance the DEMO lower port is inclined by ~20° unlike the ITER quasi-horizontal lower port, see Fig. 9. This inclination is defined by the relative vertical location of the inner divertor target with respect to the outer target, which depends on the lower triangularity of the plasma.

In toroidal direction the available space for the lower port is limited by the inner edge of the TF coils. To maximize the internal space of the lower port the lateral port walls are tapered, see Fig. 10. Within the inner contour of the TF coils toward the VV there are conflicting requirements on the port walls: if the lateral port walls are parallel, this would allow for radial assembly of the complete lower port to the main VV; however, this does not allow for enough space to connect cooling pipes to the lateral divertors. A compromise solution that meets all requirements has not yet been defined. Vertical assembly of the lower port is not possible due to the presence of the toroidal field coil inter-coil structure above the port.

5.3. Neutron and radiation shielding

In DEMO the VV currently dominates the neutron shielding. The design of the lower port, being a penetration of the VV, is therefore critical for the provision of sufficient shielding against nuclear heating to the toroidal field coils. Also streaming of gamma radiation during shutdown from the activated IVCs to the port cell where man-access may be required must be limited by suitable shielding structures inside the lower port. Hence the following adaptations of the lower port design have been introduced: (i) reduction of the lower port inclination, (ii) increase of the port wall thicknesses, in particular that of the lower port floor, (iii) integration of shield blocks behind the divertor, (iv) introduction of shield blocks in-between the TF coils below the divertor. While additional improvements are required to further reduce the shutdown dose rate (SDDR), the predicted level of nuclear heating in the superconducting coils is now sufficiently low [29].

The configuration of the DEMO lower port also separates the pipes carrying activated cooling water or lithium lead from areas foreseen for man-access during shutdown, in particular the lower port cell. This hazard piping is routed in the outer wall annex directly to the lower pipe chase below the lower port cell, see [30, 31] and Fig. 7.

6. Upper ports

6.1. Introduction

Much different to the near-horizontal upper ports of ITER, DEMO's upper ports (UPs) are completely vertical. They have to allow for the vertical movements of the BB segments during extraction and replacement. This requires a considerable size, see Fig. 1. At the same time the space available for each upper port is restricted by adjacent PF and TF coils both in the radial and the toroidal direction [6]. Each of the 16 upper ports provides access to five BB segments, the corresponding pipework and other in-port components of the respective vessel sector. More detail on the design approach and boundary conditions is given in [34].

6.1. Design input

The basis of the UP configuration development is the *DEMO 2017 design baseline* [8, 35], which has a single-null divertor configuration and integrates vertical BB segments. Thus the UP respects the space reservations of the coils. The space reservations of the magnetic coils defined therein were respected in the development of the UP configuration (as static input). The space inside the UP is sufficient for BB replacement, which was verified using flightpath models of the envisaged removal kinematics, [55]. In the future it might be considered to trade off the port size against magnet parameters (e.g. towards toroidally narrower TF coils and wider ports).

The high-level requirements of the UP configuration are summarized in Table 4.

Scope of design

The design includes the following components, to which the above requirements are flown down: port structure (part of the VV), port annex, upper limiter, neutron shield plugs, blanket chimneys and the pipework for either WCLL or HCPB blankets. This work is focused on integrating the UP with the HCPB concept because it is more challenging in terms of operating temperature, required pipe sizes and shielding. Feasible variants are investigated and a reference design option is identified.

Assumptions & choices

It is foreseen to replace the five BB segments of each sector (3 outboard and 2 inboard) at least once during the lifetime of DEMO [35]. This operation requires clearing their path from all obstructive components inside the UP, such as piping and shielding elements. In the PCD Phase, a large part of the RM activities was aimed at developing enabling technologies which are substantiated by prototyping [36]. The most relevant in-vessel operations for the upper port are the joining and disconnecting of the piping and the handling of the upper limiter, shield plugs, and blankets, pipes or pipe modules. *In-bore tools* are being developed for the servicing of pipes [37]. It should be noted that for RM tooling development, a static in-port design was used as input for integration studies, which is naturally different from the one presented here, which has much evolved since RM activities started. However, RM tooling requirements were respected in the ongoing UP design and coherence shall be achieved by reconsolidating the models in the early conceptual design phase. The design-driving assumptions with regard to RM tooling may be found in [34]. Also note that blanket handling and other RM operations need to account for failsafe transportation, rescue and recovery [38].

The piping presented here represents a *concept choice*, i.e. seamless pipes with suitable layout and dimensioning to sustain operational loads and provide a degree of compliance to enable installation. The *complementary concept* was developed in parallel by the RM project using flexible pipe elements under cyclic, high pressure internal loads, thus limiting piping stiffness [36].

6.2. Design description and rationale

The upper port design has single-shelled toroidal walls to maximize the space inside the port. These were structurally verified for critical load cases [39]. The piping of all in-vessel clients is routed radially through 16 upper port annexes to the upper pipe chase in the tokamak building, see Fig. 11. The vacuum boundary to the in-building air side is the penetration plate. It is located at the very end of the annexes (on the

Table 3
Types of lower port currently considered.

Function	RH port	Pumping port	Pumping + RH port
RH	Divertor replacement Divertor and BB pipe servicing	Remove & replace the torus vacuum pump RH access to service divertor and BB piping	Divertor replacement Removal & reinstallation of the torus vacuum pump Divertor and BB pipe servicing
Vacuum pumping	no	Provide pumping path to the main plasma chamber and host the torus vacuum pumping unit	
Pipe routing	4 cooling pipes per divertor cassette 1 LiPb pipe per BB segment		
VV support	yes		
Neutron shielding	Shield plug behind divertor possible	Open pumping path causes high neutron streaming into lower port	

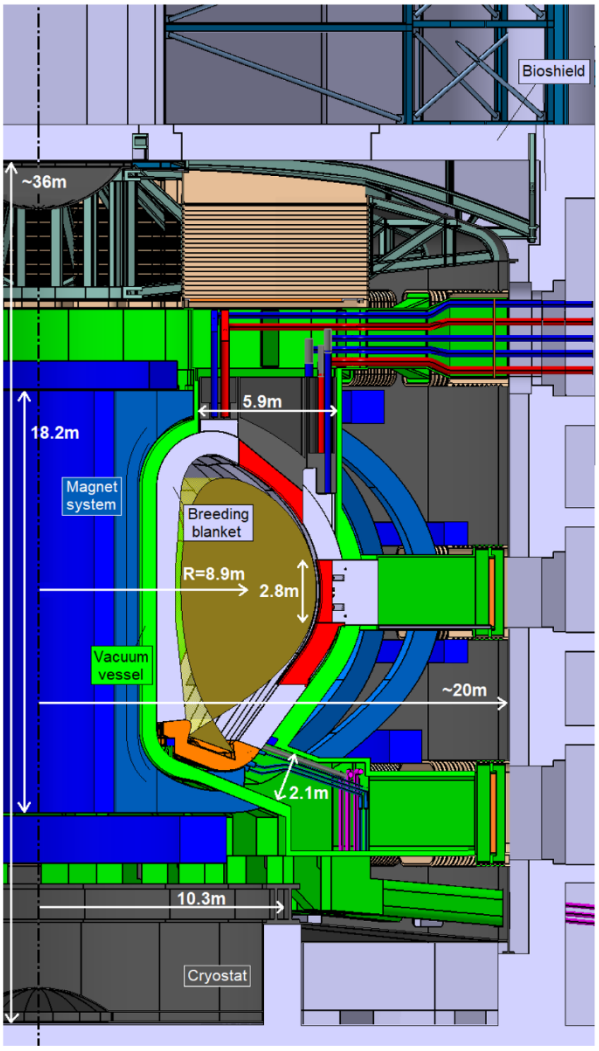

Fig. 1. Section view of the DEMO tokamak with upper and outboard limiters (red). For main dimensions of VV and IVCs see [8].

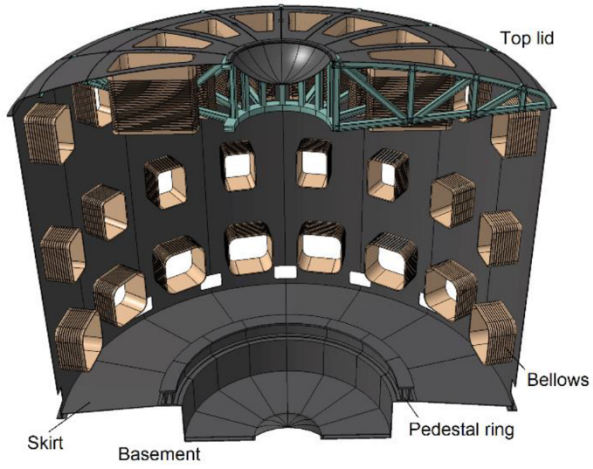

Fig. 2. Cryostat with basement, pedestal ring, skirt, main cylinder, top lid with radial girders, and bellows (T-stiffeners on main cylinder not shown).

Table 4
High-level requirements of the upper port.

Requirement	Comment
Maintenance: Enable in-VV access and BB removal	Baseline 2017 port contour is used. (Verification was done with a CAD flightpath model, future optimization however possible)
Shielding: Limit peak nuclear heating in all coils <50 W/m^3	Port-adjacent TF leg is most critical.
Shielding: In-cryostat SDDR to allow occasional man-access, target: 100 μSv/h [8]	Remark: SDDR depends only partly on the UP design (requirement shared with other ports, VV etc.)
Wall protection: Integrate upper limiter (UL) & enable quick replacement	The upper limiter protrudes the BB first wall to protect it from impact of charged particles [5, 8]. For quick replacement the UL is designed as a non-captive component (incl. service pipework)
Safety: UP shall be a safety and vacuum barrier	The UP is a part of the VV and designed according to the same regulations

low field side) to increase in-vessel pipe compliance (by length). The annexes are located in the toroidal center of each vessel sector. They act as "guard pipes" shielding the in-cryostat environment from heat and nuclear radiation and providing protection in case of leaks.

Below the level of the port closure plates and above the upper arc of the TF coils, all 16 upper ports are connected forming the upper ring channel, see Fig. 11. The size, in particular the height, of this ring volume is mainly driven by the pipe layout within the port. The upper ring channel constitutes a single volume of ~1500 m^3. This offers a much larger expansion volume than individual ports, which is beneficial for pressure suppression in case of a pipe rupture. It also provides space for the integration of radial pipes outside the extraction path of the limiter plug and thus can remain in-situ during limiter RH.

The in-vessel primary coolant piping features *temporary pipe modules*, which need to be removed prior to removal of the blankets. These service an entire BB segment each, i.e. comprise lines for coolant, tritium extraction (HCPB: purge gas; WCLL: liquid metal) and small service vacuum system (SVS) lines for interspace monitoring and weld gas supply. The pipe modules interface with the BBs using an in-situ, in-bore welded (and cut) connection. At the interface to the permanent piping of

the port annex either mechanical pipe connectors (MPCs[1]) or welding is used. An overview of the pipework associated with the HCPB BB is shown in Fig. 12 for the MPC option. The water supply for the shield plugs and the upper limiter is shown in green. It should be noted that these lines are the only components to be removed to allow vertical extraction of the upper limiter, which is mounted underneath the central port plug, see Fig. 1.

The UP plug is segmented into three radial components: inboard, central and outboard plug, see Fig. 13. The in- and outboard plugs embrace the BB piping for better shielding and are thus captive. The central plug has a load-bearing function, mechanically interfacing with both the COBS and both inboard BBs. More details may be found in [34]. The limiter, composed of a plasma-facing unit and a Eurofer shield block, see [41], is mounted underneath the central plug. It protrudes by ~70 mm with respect to the first wall (FW) through the blankets, to which it has a gap of ~20 mm at its lateral faces for insertion clearance and to remain force-free except for unavoidable loads (EM, inertial, internal pressure).

6.3. Verifications

The requirement on the UPs to provide sufficient space for blanket replacement is met a priori through adoption of the 2017 baseline geometry. The same holds for the clash-free integration with the magnets while reserving sufficient space (100 mm) for future integration of the VV thermal shield. The following requirements were verified by analysis for the UP configuration:

1 Shielding to achieve nuclear heating < 50 W/m^3 in the TF coils: Maximum values produced by dedicated MCNP analyses are 17 W/m^3 for the HCPB configuration and 22 W/m^3 for the WCLL model, respectively.
2 SDDR – WCLL (Fig. 14): MCNP calculations yield a sufficiently low in-cryostat gamma radiation level during maintenance in the vicinity of the UP. Note: Any SDDR contribution from water activated during operation is expected to be insignificant and was therefore neglected.
3 SDDR – HCPB (Fig. 14): MCNP calculations show that *significantly thicker* UP walls (~300 mm) would allow reducing the SDDR level inside the cryostat to 1000 μSv/h, which approaches the target value.
4 Stresses of in-port BB pipes: The BB piping was verified by FE to sustain the internal coolant pressure load with sufficient flexibility to accommodate the thermal expansion of both the BB segments and the pipes during operation. While the thermal stresses in the larger HCPB pipes are close to the limits, the smaller WCLL pipes have larger margins [40].
5 Upper port annex: The upper port structure was verified by FE to withstand the bending loads during seismic events.

6.4. Conclusions & outlook

The configuration of the upper port including the integrated design of the main in-port components, namely shielding plugs, pipework and plasma limiters has been developed. It was successfully verified by analysis for most of the main risks perceived as concept critical, including in-pipe stresses and neutron shielding. A systematic design approach ensuring traceability of decisions was used, including the documentation of assumptions with relevance to results (e.g. gaps versus shielding performance).

The nuclear heating in the magnets is sufficiently low in the current configuration. The in-cryostat SDDR target is marginally met for the WCLL BB concept. For the HCPB, larger pipe diameters require larger penetrations in shielding structures and the coolant is transparent to neutrons. Both leads to more pronounced neutron streaming into the UP. This conceptual shielding flaw could be resolved by adding large amounts of shielding material to the upper port walls.

The developed piping layout allows non-captivity of the limiters, and the space it requires is one of the reasons for connecting all UPs to form the UP ring channel, a major feature of the UP configuration. MPCs might be used for the interface of the temporary pipe modules to the permanent in-port piping, while the interfaces to the BBs are foreseen to be welded.

The high stiffness of the seamless coolant pipes requires high installation forces depending on geometrical tolerances still to be studied, even with the "omega" features included. The outcome of appropriate prototyping may motivate the integration of flexible pipe elements, if deemed less risky. In the subsequent Concept Design (CD) Phase of DEMO, a dedicated pipe test facility will likely be needed for proper development and risk & benefit evaluation to substantiate piping concept choices. In the greater context, the input conditions accepted as fixed in the present work should also be revisited, namely the space reservations of the magnets, the BB extraction space envelope, the number of TF coils and possibly others.

7. Equatorial ports

7.1. Generic configuration

DEMO has 16 equatorial ports. As a working basis four out of these are reserved to incorporate plasma limiters, six for the installation of the electron cyclotron (EC) system, and the remaining six for the integration of other heating and diagnostic systems. The equatorial ports incorporating plasma limiters provide access to outer midplane limiters (OML), outboard lower limiters (OLL) and inboard midplane limiters. Thus four of each of these limiters are considered, see also [42]. Upon removal of the limiters the equatorial ports also provide access into the VV for the multipurpose deployer [43, 44].

The DEMO equatorial ports were initially foreseen to be in the center of two adjacent TF coils as in ITER. However, since in DEMO each sector has 2 inboard and 3 outboard BB segments, this would have led to a central outboard segment being divided into two halves. In order to avoid this, each of the equatorial ports is shifted toroidally and slim rectangular cut-outs are integrated into two adjacent BB segments, with a maximum of one third of their toroidal width. Thus the penetration of the BB by the ports plugs (which is the case for the limiter) or the openings (which is the case for the EC system) is possible, see Fig. 15. The reduction of the tritium breeding performance of the BB due to the required cut-outs has recently been found tolerable [33].

7.2. Outer midplane limiter port

Four equatorial ports are currently foreseen for the integration of the OML [32]. During ramp-up, before the x-point is established, the plasma is in contact with this limiter for edge definition and particle exhaust.

7.2.1. OML design requirements

As initial design inputs, the following requirements were defined: the OML must protrude past the BB FW by 20 mm. The mutual alignment between the four OMLs shall be ±1 mm (based on the toroidal field axis and the 5 mm scrape off-layer (SOL) power fall off length λ_q during ramp-up) to enable adequate power sharing amongst the four limiters. To achieve this precision an active alignment is needed since the installation precision with respect to the TF axis is expected to be no better than ±2.5 mm, see Fig. 15.

The number and size of the OMLs needs to be chosen in order not to exceed the heat load capability of its plasma-facing components (PFCs). A toroidal width of ~1.1 m and a poloidal height of ~2.7 m was found sufficient in this respect in preliminary studies [42].

Two separate cooling circuits are presently considered to allow the

[1] Note that the pictured MPCs are in the open position (flange clamp disengaged). This is to determine the total required space in the CAD model.

operation at individual temperature levels of the PFCs (at ~140 °C) and the shield block (at >180 °C), respectively.

Like other DEMO port plugs the OML must sufficiently reduce the neutron flux to prevent excessive heat loads on the superconducting coils (<50 W/m^3) and to allow personnel access during maintenance into the cryostat and to the port closure plate (SDDR <100–1000μSv/h 12 days after shut-down), [8].

7.2.2. OML port and port plug design

The PFCs are mounted on the shield block, which is a box structure filled with stacked steel plates for neutron shielding, see [41]. Both are cooled by water to moderate the neutrons. The shield block is made of the reduced activation steel EUROFER to minimize rad waste. The shield block is mounted on the port plug and can be replaced together with the PFCs at the end of its lifetime or in case of failure. The limiter shield block in the current design weighs ~4.5 tons. The associated port plug made of austenitic steel is expected to weigh ~12 tons.

The OML port with integrated limiter port plug is shown in Fig. 16 with radial actuator and interfacing components. The four cooling pipes and the services for the actuators and sensors are routed permanently on the port sidewall outside the port plug extraction path. They penetrate permanent parts of the primary vacuum boundary but not the port's vacuum closure plate. To facilitate the handling in the active maintenance facility (AMF), lifting features are integrated in the top. The shield block can be replaced in the AMF after release of the vertical and radial fixations as well as of the cooling pipes via lateral access.

In the configuration shown in Fig. 16 the vacuum closure plate is far behind the port plug. This had been chosen to avoid the vertical space constraints given by the poloidal field coils PF3 and PF4 and hence provide more space to access the port closure plate and the cask docking flange. A concept is yet to be developed to pump out the volume behind the port plug during the dwell period between plasma pulses. Either sufficient vacuum conductance needs to be implemented between the VV and the port plug or a local pumping system has to be considered.

Small nominal gaps (10 mm) are implemented around the OML port plug to the VV to minimize neutron streaming. For further reduction a dog-leg is included. The gaps around the PFCs and the shield block to the IVCs are affected by the relative thermal expansion between the VV and the BB of ~10 mm as well as the expected fabrication and installation tolerances. The gaps must prevent physical contact to avoid electrical currents to flow between the limiter and IVCs. In operation the following nominal gaps are expected:

- At the top ~20 mm to the BB
- At the toroidal sides ~20 mm to the BB
- On the bottom ~10 mm to the OLL

7.2.3. Mechanical supports and radial alignment

Large EM forces and moments may act during operation, in particular during plasma disruptions. The port plug is mechanically fixed to the VV port by a bolted flange much like the ITER port plugs. The shield block is mechanically fixed to the port plug such that it can be replaced in the AMF within reasonably short time. A set of shear keys and hinge supports is used to transfer all loads to the port plug, see Fig. 17. Features are included so that the shield block is radially adjustable with respect to the port plug.

The pneumatic actuators which move the shield block into its precise position are based on a piston - spring concept where an applied pressure acts against a spring force, thus defining the position of the piston [32]. The assembly is encapsulated by bellows. This type of mechanism is used for the mirrors of the ITER electron cyclotron launchers but with much smaller dimensions [45]. The OML can be radially adjusted when the TF is off and the high ferromagnetic forces that act on the EUROFER shield block during operation (~1.5 MN) are not present. A locking unit (brake), which can cope with all the anticipated forces, fixes the actuator position during operation.

7.2.4. Neutron shielding

To meet the radiation protection criteria, see above, the OML must sufficiently reduce the neutron flux. This will protect the superconducting coils and hence also limit the activation of the steel in the maintenance areas ensuring a sufficiently low gamma radiation level during maintenance. In addition to the shield block the front part of the port plug incorporates steel plates similar to those of the VV, see Fig. 3, which further reduces the neutron flux. A dog-leg was introduced into port plug and VV to limit neutron streaming in the gap, see Fig. 17.

Monte-Carlo N-particle (MCNP) simulations were undertaken to assess the nuclear heating in the superconducting coils and the gamma radiation level during maintenance both in the cryostat and on the outside of the vacuum closure plate, see Fig. 18. The peak value of the neutron heating in the magnet coils in the vicinity of the OML port of 20 W/m^3 is well below the limit (50 W/m^3). Also the target values for the SDDR in the maintenance areas are met. However, in this early phase of design gamma radiation contributions from other ports were not considered. A more comprehensive MCNP model will be used in the future to capture such effects. Further improvements of the radiation shielding structures of the OML port may therefore be necessary.

7.2.5. Conclusions and outlook

Based on the requirements collection the design of the OML was engineered including a cooling concept and an actuator with brake. The integration into the tokamak and the port layout was developed. The port closure plate may be shifted closer to the port plug in the next development phase. Optimizations of neutron shielding capabilities will further reduce the shutdown dose rates in the cryostat and port interspace. This is also required to cope with cross-talk from other ports. The alignment mechanism and locking unit are to be further detailed. Tokamak and building integration considering also space reservations for the remote maintenance tools, has been done initially and needs to be refined further. A final choice has to be made on how to connect / disconnect pipes (by cutting/re-welding in-bore or orbital and/or a combination with mechanical pipe connectors).

7.3. EC launcher port

7.3.1. Design requirements

Currently, it is assumed that all heating and current drive functions are provided by the EC system alone. The maximum EC power available during flat top of ~130 MW is assumed to be composed of ~30 MW for bulk heating, ~30 MW for the control of neoclassical tearing modes (NTMs), and ~70 MW for the control of radiative instability [46]. Few configurations of the EC system were studied aiming for a high availability. A promising option proposes to install - with some redundancy - 108 gyrotrons, each providing a power of 2 MW at frequencies of 170 GHz and/or 204 GHz, respectively. Both, gyrotrons operating at fixed frequencies and gyrotrons with tunable frequencies are feasible with this design concept. From the gyrotrons the EC millimeter-wave power of maximum 130 MW will be transmitted into the plasma by 108

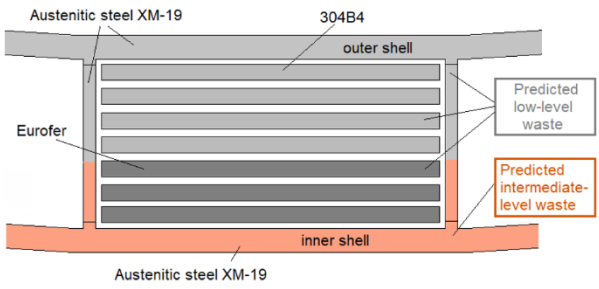

Fig. 3. Section of the VV double wall structure with in-wall shielding plates (inboard) and indication of materials selected for different components and expected activation waste classification (not to scale).

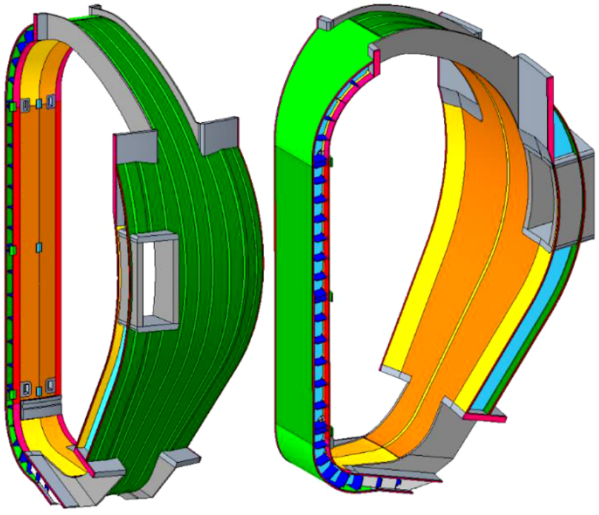

Fig. 4. Design of one sector of the DEMO VV with port stubs (gray) and splice plates (red) (IVC supports on the outboard not shown). Welds are present at the interfaces of differently colored surfaces.

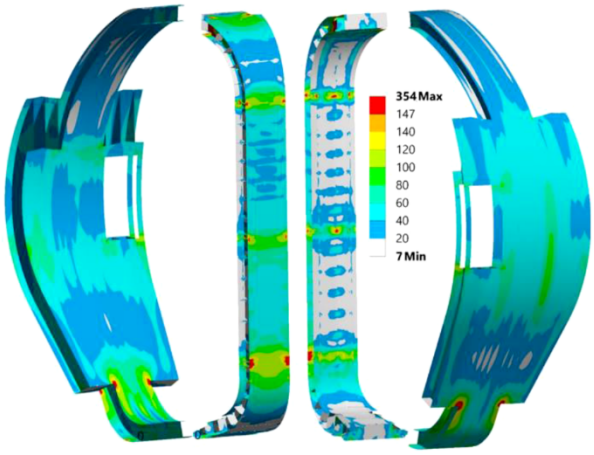

Fig. 5. Elastic membrane stresses in the VV [MPa] due to the application of dead weight, coolant pressure, EM loads during a TFCFD, and interface loads on the IVC support structures.

transmission lines, which are integrated into six equatorial ports [47, 48]. Other variants with a different number of ports were studied but are either occupying too many ports or could not achieve the system availability. A final choice of the number of ports will be made in the CD Phase. The EC beam launching points were defined considering plasma heating and current drive requirements. Each function was elaborated in dedicated studies resulting in an EC port plug design that was verified by recent physics studies [46].

7.3.2. EC port and port plug design description

Each EC port plug integrates four groups of waveguides that are arranged one on top of the other. Two groups are installed in the upper and lower part of the port plug with three waveguides per group that are used to control NTMs. Two additional groups are installed in the center of the port plug with eight waveguides per group for bulk heating and radiative instability control, see Fig. 19.

As in the case of the outer midplane limiter, the EC launcher penetrates the BB in-between two adjacent segments to maintain the vertical integrity of the BB segments, see Fig. 15. Thus the port was shifted from the sector center to a lateral position, see Fig. 20. Through the arrangement of the fixed and the steerable mirrors a dogleg structure is created inside the port plug which reduces the streaming of neutrons.

For the variant based on gyrotrons with fixed frequency the port plug is divided into two separate parts, the fixed mirror EC plug and the steering mirror EC plug, see Fig. 20. This modular concept allows the integration of all steerable mirrors in one port plug that can be maintained independently from the other accounting for the different lifetimes of the two plugs:

- The steerable mirrors with actuators that face the plasma require regular replacement due to material degradation similar to the divertor or the limiters. They are also expected to be more prone to failure, The arrangement of the steerable mirror plug allows its removal without removing the waveguide bundles.
- The fixed mirror plug instead is somewhat protected from the neutrons by the BB segments. It also integrates no movable parts. It is therefore aimed at optimizing the design such as to make it a lifetime component requiring replacement only in case of unexpected failure.

The front modules of both plugs are currently assumed to be made of EUROFER given its neutron irradiation resistance and reduced activation properties. Also the base of the mirrors is assumed to be made of EUROFER and coated with tungsten. The DEMO steering mirrors have approximately ten times the surface area as compared to those of ITER [45, 50, 51]. The actuator system has therefore been designed for higher loads and taking into account the higher microwave power loading per mirror due to the larger number of beams.

For the variant based on gyrotrons with tunable frequencies the same design could be used, adapting the formerly described steerable mirrors to a fixed location without actuators and instead tuning the gyrotron frequency to steer the EC absorption location.

During in-vessel maintenance both plugs can be moved radially on rails, see Fig. 21. They weigh ~40 tons (steerable mirror plug) and 30 tons (fixed mirror plug), respectively.

7.3.3. Neutron shielding

The large beam openings allow the neutrons to penetrate deep into the port plug and compromise its neutron shielding function. Several iterations were made progressively reducing the neutron streaming through the EC port. Dogleg structures were implemented for the mirrors and also between the two port plug segments. In addition large auxiliary shields behind the fixed mirror were added to the design to reduce the neutron flux and thus the SDDR during maintenance. In spite of these efforts the SDDR values inside the cryostat remain high at ~1000–10,000 μSv/h Fig. 22, a level that is approximately one order of magnitude above the criteria. Further design optimizations are therefore required in the future.

At the same time neutron transport calculations showed that the design improvements implemented so far, including thickening of the shielding walls meet the nuclear heating limit of the superconducting coils.

7.3.4. Outlook

The main focus for the EC port development in the CD Phase of DEMO is the further elaboration of the sub-systems, e.g. the mirror actuator, as well as a more detailed load assessment and structural integrity verification. Mockups of the actuators should support the design process. Further improvement of the neutron shielding structure should reduce the SDDR sufficiently. This also requires consideration of the cross-talk from other ports to get more realistic values. Since the physics basis is still not yet fixed, a permanent change of the design might be the consequence if the functions, required power levels and/or beam absorption region etc. changes. Therefore the design has to cope with such uncertainties and be prepared for them.

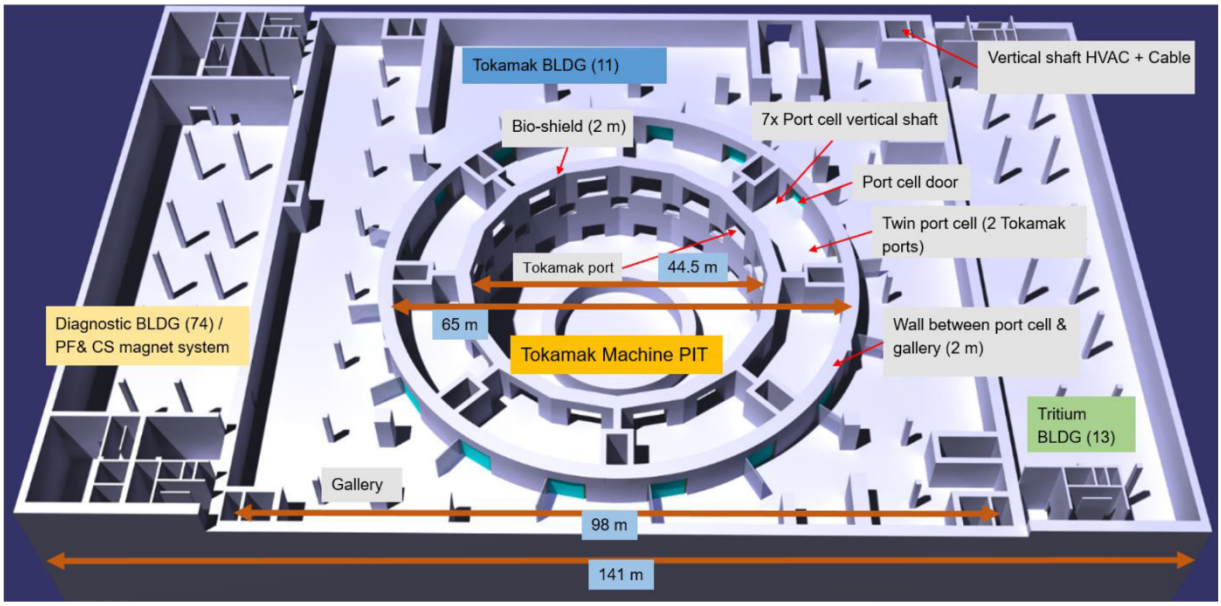

Fig. 6. DEMO tokamak building level associated to VV lower ports (B2 level).

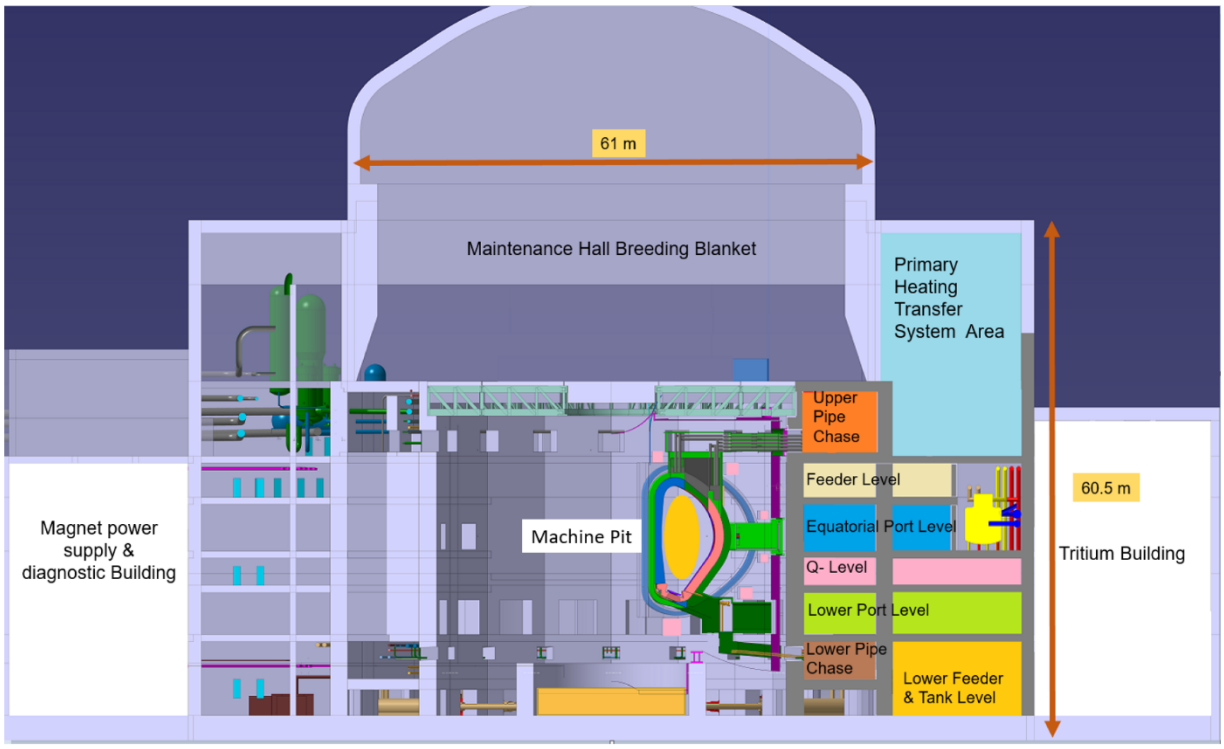

Fig. 7. Tokamak complex level arrangement (non-self-supported cryostat shown).

8. Breeding blanket mechanical supports

8.1. Introduction

A tokamak architecture based on large vertical blanket segments was – to the authors' best knowledge - first considered in the early 80 s in INTOR [52] and later adopted in NET [53] and the European power plant conceptual studies [54]. This architecture aims at reducing the number of IVCs and hence the duration of their replacement and allows the use of a crane-like device to lift the heavy BB segments. The NET team eventually abandoned vertical blanket segments, partly because of difficulties encountered in the search for an attachment concept.

The basic principle of the BB attachment concept that is presented here was first introduced in [8], is described in further detail in [55] and has been partially verified in [56] considering electromagnetic (EM) loads assessed in [57].

This section:

i Introduces the requirements and principles of the BB support concepts,
ii Defines the relevant machine states,

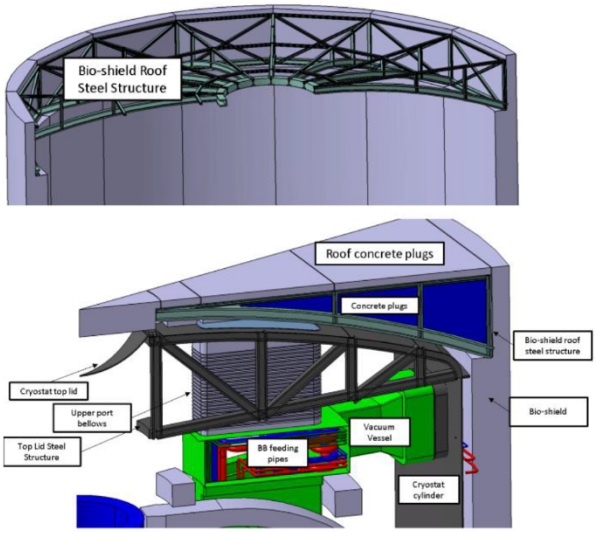

Fig. 8. Top: bioshield roof structure supported on bioshield. Bottom: configuration with cryostat, cryostat bellows and VV.

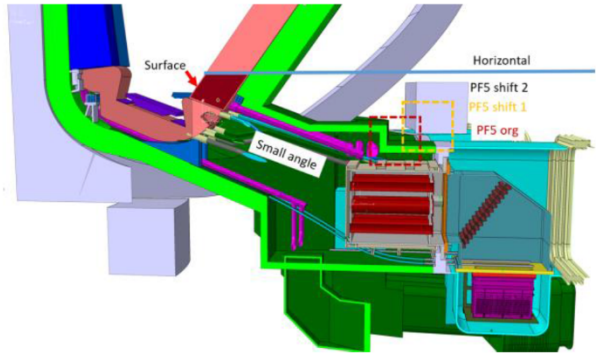

Fig. 9. Vertical cross-section of the lower port (green) with port duct (cyan), BB pipes (pink), divertor pipes (gray), metal foil pump (red) and diffusion pump (pink).

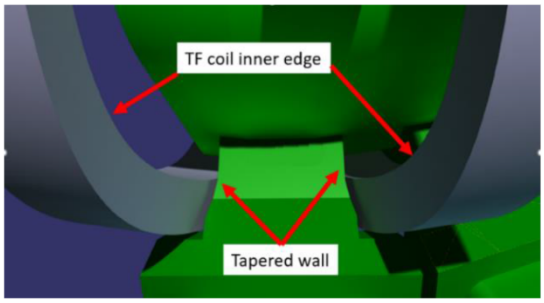

Fig. 10. Radial view from the cryostat onto the lower port between two adjacent TF coils.

iii Describes the design of the individual BB supports, their final tolerances and the expected BB positioning precision,
iv Summarizes the BB load conditions, and
v Presents the results of the structural assessment.

8.2. Requirements

The main requirements to be met by the BB attachments are:

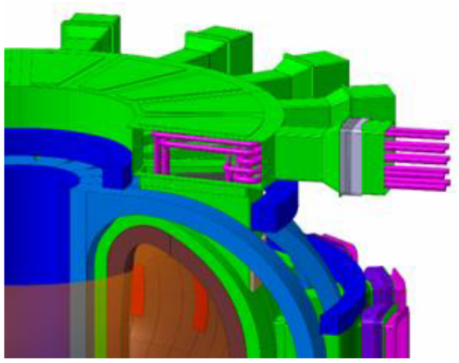

Fig. 11. Upper port general layout with the UP "ring channel" and the 16 UP "annexes" connected to the cryostat via bellows (gray) and housing all piping of in-vessel clients.

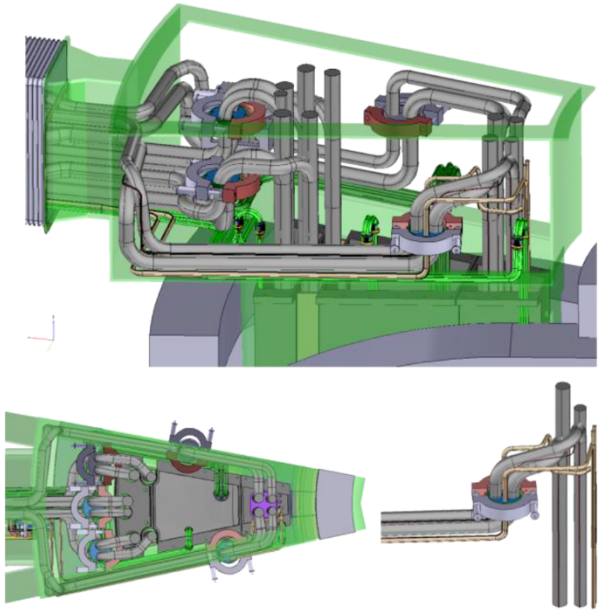

Fig. 12. Upper port internal pipework (HCPB option). Detail: Inboard BB pipe module (bottom right) with MPC, pipes for He-coolant & monitoring and pipe stubs for in-bore tool access on top.

- To withstand all loading conditions and accommodate all thermal states of the BB, see paragraph 8.9.
- To provide accurate alignment of the BB FW to avoid heat load concentrations due to charged particles, e.g. on leading edges, see also [58]. Since protection limiters are foreseen in DEMO that will protrude beyond the BB FW and therefore collect most of the charged particles flowing essentially along the magnetic field lines, we expect the FW alignment requirement to be reduced compared to that of ITER.
- To provide proper electrical connection of the BB to the VV, see [8].
- To enable installation of the BB segments by the provision of guiding features requiring from the BB transporter a BB positioning precision of ~±40 mm prior to the final engagement
- To enable release of the BB segments by the choice of appropriate surface coatings to prevent stiction in vacuum, e.g. Al-bronze pads with a 250 μm thick plasma-sprayed alumina coating [59].

8.3. Mechanical support principles

Each blanket segment is individually supported by the VV without any physical contact to the other blankets or IVCs. All BB support

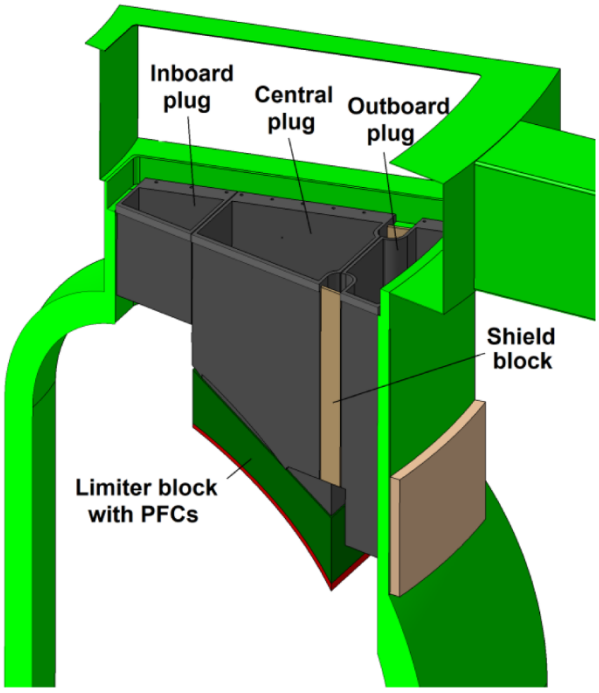

Fig. 13. Shield plugs (dark gray), upper limiter shield block (dark green) with plasma-facing components (red), and B_4C shield blocks (brown) in the upper VV port (green).

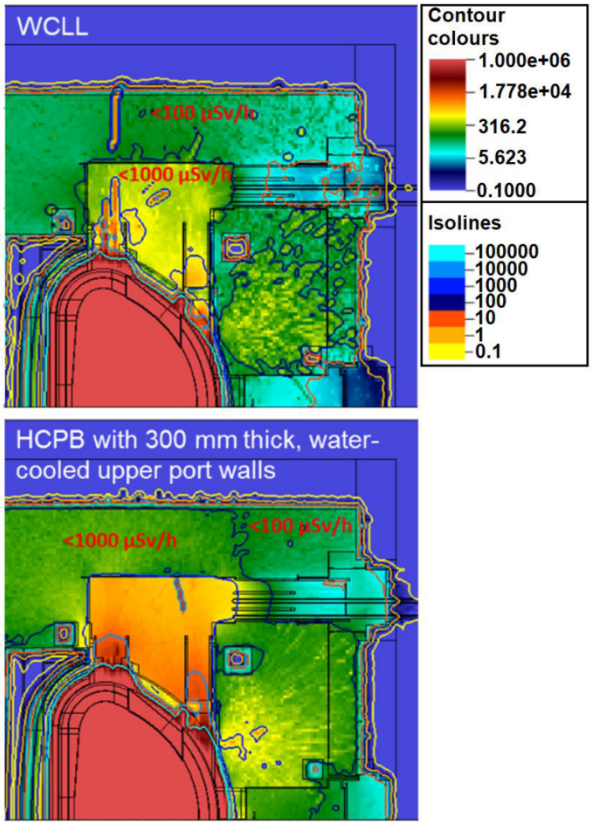

Fig. 14. Upper area dose-rate maps 12 days after plasma shutdown, WCLL blanket option (top), HCPB option with thickened, water-cooled UP structure for better shielding (bottom). Note: other ports artificially closed to avoid interference in the results, i.e. no cross-talk.

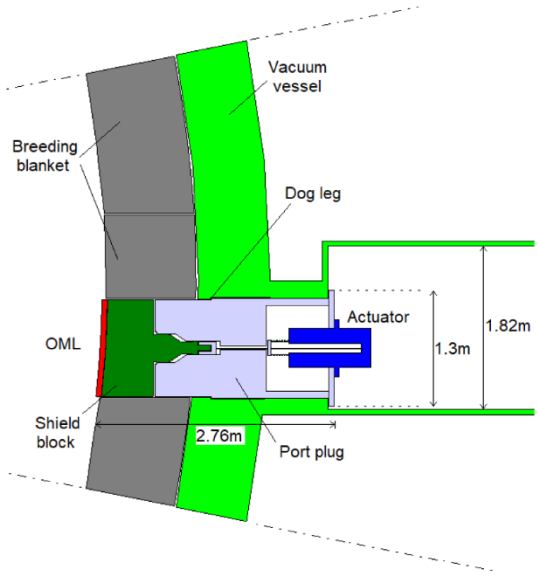

Fig. 15. Horizontal cross section of the OML integrated in the equatorial port that is toroidally shifted to the division line between the central and a lateral outboard BB segment.

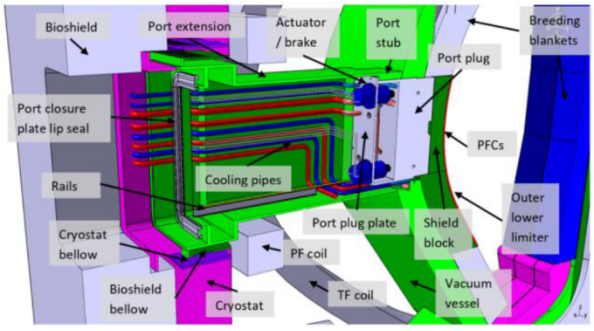

Fig. 16. OML port design (poloidal cross section, isometric view).

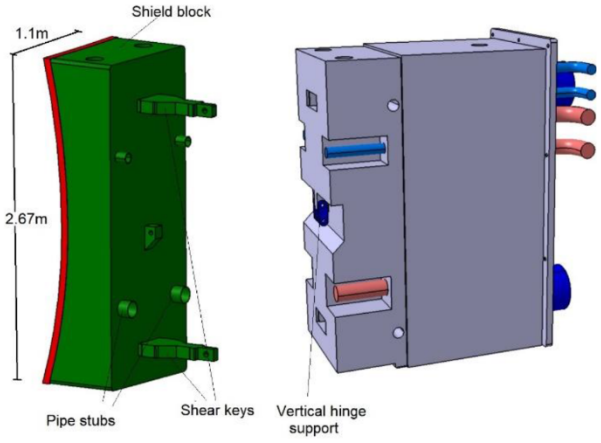

Fig. 17. Left: shield block (green) with PFC (red) and mechanical interfaces. Right: Port plug (gray) with cooling pipes (light red and light blue) and actuators (blue).

structures are shear keys or contact pads relying on simple compressive contact for load transfer; bolts or pins are not used to simplify the remote maintenance operations required for the BB replacement. To support the inboard segments against the very large radial loads radial supports are

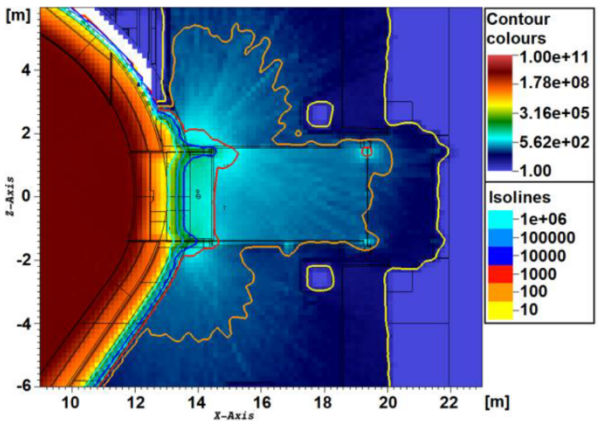

Fig. 18. Shutdown dose rate 12 days after plasma shutdown in the vicinity of the OML port during maintenance [μSv/h]. The lower and upper ports are artificially closed in the simulation to avoid interference appearing in the results due to other sources, i.e. no cross-talk is accounted for.

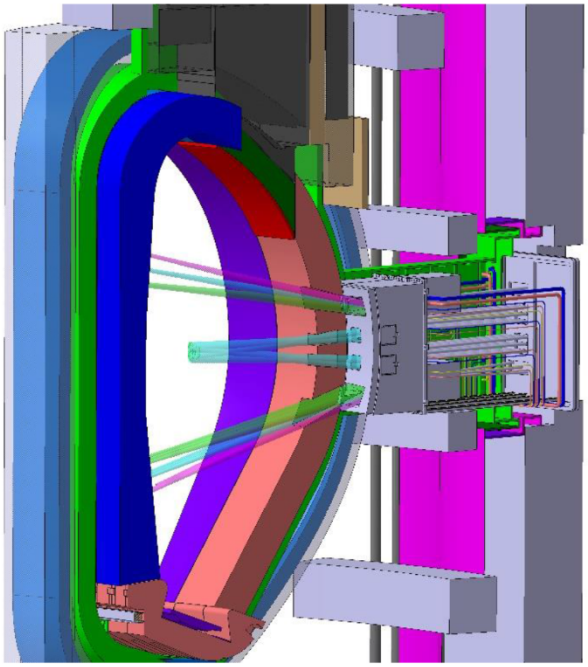

Fig. 19. EC port plug with EC beams, poloidal cross section view, [49].

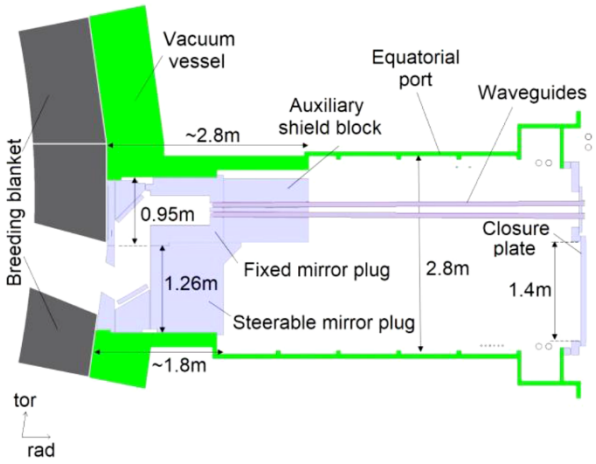

Fig. 20. Horizontal cross-section of the EC port.

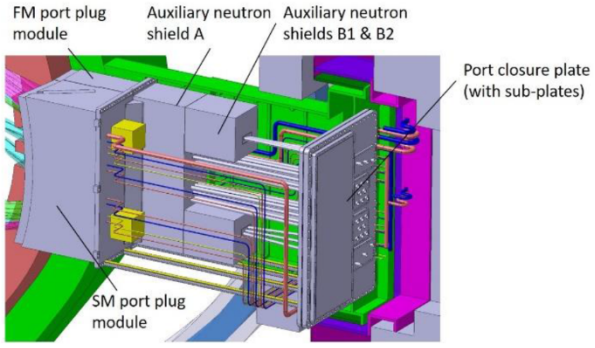

Fig. 21. View into the EC port.

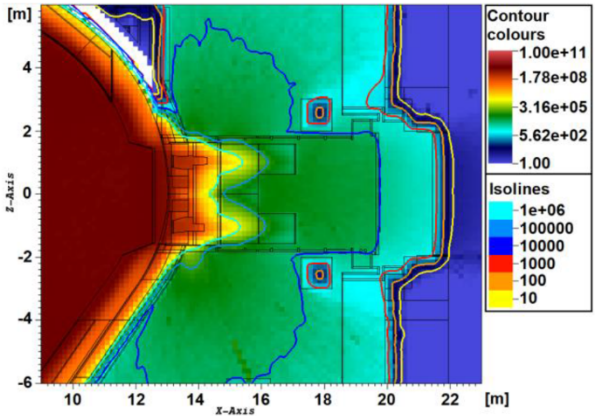

Fig. 22. Shutdown dose rate 12 days after plasma shutdown in the vicinity of the EC port [μSv/h]. The lower and upper ports are artificially closed in the simulation to avoid interference in the results due to other sources, i.e. no cross-talk is accounted for.

incorporated at three poloidal locations. The outboard segments are radially supported only at the top and at the bottom. During tokamak operation the BB segments are radially pre-compressed by the ferromagnetic force and vertically pre-compressed by obstructed thermal expansion. a) Radial pre-compression by the ferromagnetic force

The radial gradient of the TF generates a large radial force on the ferromagnetic blanket material EUROFER. Since the TF is constant during and in-between plasma pulses, during tokamak operation the BB support concept can rely on this force to guarantee physical contact at the radial supports with significant pre-compression. As a consequence bolts providing pre-compression as e.g. in the supports of the ITER blanket [59] are not required.

The structural concept of the BB segments attachment is that of an arch bridge where both end points of the arch are constrained. When there is a temperature rise, the bow of the arch is sufficiently flexible to increase and reaction forces on the supports remain tolerable. The radial ferromagnetic force acting on the blankets corresponds to the vertical gravity force acting on the conceptual bridge, see Fig. 23, and also defines their radial position. Horizontal slits incorporated in the BB FW and breeder zone as in the previously envisaged multi-module segment design concept [60, 61] are not required. The curved part of the otherwise straight inboard segment provides sufficient bending flexibility if the upper vertical support is located at the end point of the segment. Otherwise it would be too stiff if constructed as a single box structure with a poloidally continuous FW plate and its thermal expansion would cause a steep rise of the vertical reaction forces [56].

It had initially been assumed that during operation the ferromagnetic

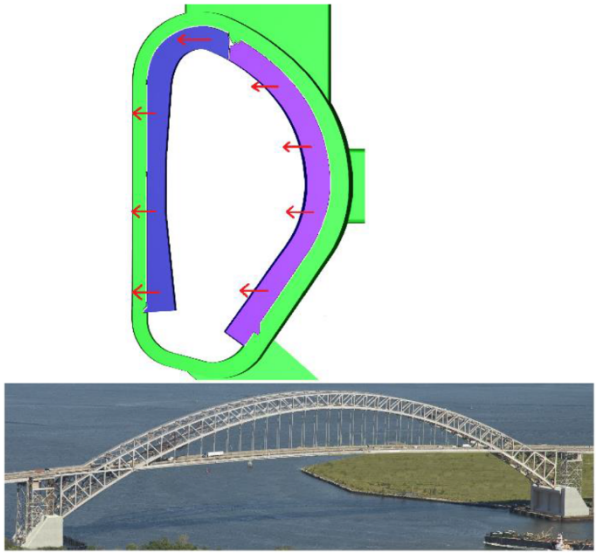

Fig. 23. Top: attachment concept of the vertical blanket segments relying on the presence of radial ferromagnetic forces (red arrows). Bottom: New Jersey Bayonne bay arch bridge relying on Gravity.

force would ensure physical contact on the radial supports of the blanket segments in all load cases. Instead it was found that EM forces due to a plasma thermal quench, a fast plasma current quench and due to a fast discharge of the TF coils may exceed the ferromagnetic force on some BB segments [55]. Consequently the BB segments must be supported at the top and at the bottom in both radial directions. This fact also disqualifies the radial supports from being used as electrical connection to the VV as the electrical configuration would become unreliable. Instead we rely on the vertical supports for electrical connection. The radial supports will be electrically insulated, see Section 8.2. b) Vertical pre-compression by obstructed thermal expansion

After installation of the BB segments a small gap remains at their upper vertical supports that will close due to the thermal expansion of the segments when preheated to 300 °C in *standby* state. Hence prior to plasma ramp-up the BB segments are vertically clamped between their upper and lower vertical supports. During plasma operation the clamping force will further increase as the plasma-facing areas of the BB heat up more than the back side. Thus physical contact between VV and BB is guaranteed and the vertical supports can be relied upon for electrical connection.

At the same time the BB segments are not free to thermally expand and their temperature state causes (secondary) stresses within the BB and reaction forces on the BB vertical supports. The potential for these reaction forces to overload the BB supports thus requires controlling the BB's stiffness and its temperature levels in normal and upset conditions, see paragraph 8.9. c) Supports in shutdown state

At machine shutdown the TF coils are discharged and the ferromagnetic force no longer acts. The BB cooling systems are either idle or operate at low flow and at much reduced temperature. The BB segments will have thermally contracted and lost contact at their upper vertical supports. Consequently, the support constraints are different: the BB segments are vertically supported at the bottom and toroidally constrained by shear keys. Radial stops at the upper vertical supports prevent the BB segments from falling off the VV wall due to the location of their centers of gravity or during a seismic event.

8.4. Electrical connections

The electrical connections between VV and BB rely on physical contact of the corresponding metallic surfaces that is provided by the vertical pre-compression due to the BB thermal expansion. Electrical connections between BB and VV being both at the top and bottom avoid halo currents inside the BB segments from flowing poloidally from the top to the bottom or vice versa.

8.5. Machine states and fabrication tolerances

The gaps around the BB segments are rather small (~20 mm). Also the clearances at the supports must be small during operation to avoid dynamic amplification of the large EM loads acting on the BB, typically not larger than ~0.5–3 mm depending on the relevant BB natural frequency [62, 63]. Given the BB's considerable dimensions and temperature variations, see Table 5, the scale of its relative thermal expansion to the VV is similar and - in some cases – exceeds the dimensions of these clearances. A number of machine states must therefore be considered in the definition of the BB support concept to control the clearances and also to avoid excessive reaction forces due to obstructed thermal expansion.

The reasonably achievable shape tolerances of the BB and the VV are expected to lie in the range ±5–20 mm based on fabrication experience of the ITER VV [68]. These are larger than the required precision of the clearances at the BB supports. It is therefore foreseen to custom-machine the BB support contact surfaces after fabrication and survey as applied on the contact pads of the outer intercoil structure of the JT60SA magnets [69]. A final precision in the mm and sub-mm range is expected.

8.6. Design of the supports structures

8.6.1. Radial supports

Radial supports are implemented in all cases on both lateral sides of the BB segments, see Fig. 24. During operation the ferromagnetic force provides a pre-compression on two lateral radial supports at three poloidal locations on the inboard and the outboard segments, respectively. Due to the pre-compression provided by the ferromagnetic force they can support the BB segments also against vertical moments that may occur in plasma disruptions.

8.6.2. Toroidal supports

In addition to radial/vertical supports each blanket segment has toroidal shear keys that engage with corresponding slots in the VV. These shear keys react the large radial moments acting on the blanket during a fast plasma current quench in a disruption. Two shear keys, one at the bottom and one at the top, provide a statically determined support condition.

8.6.3. Radial stops - inboard segments

Inboard and outboard segments are radially supported also towards the outboard side. Contact pads on the VV inner shell will support the outboard segments. The inboard segments will be supported against forces pulling them off the VV wall by a radial stop of 30 mm height integrated into the upper support rail supports, see Fig. 25.

Table 5
Toroidal field, VV and BB temperatures in different machine states.

State	TF	T_{VV}	T_{BB}
IVC	OFF	20 °C	20 °C
installation			
Baking	OFF	180 °C	240 °C
Standby	ON	~50 °C	300 °C
Flat top	ON	~50 °C	~[300–500 °C], [64]
Ex-vessel	ON	~50 °C	~[300–585 °C] (initially), [65] ~550 °C (after
LOCA			~1 h), [66]
BB	OFF	20 °C	~[50–80 °C], [67]
maintenance			

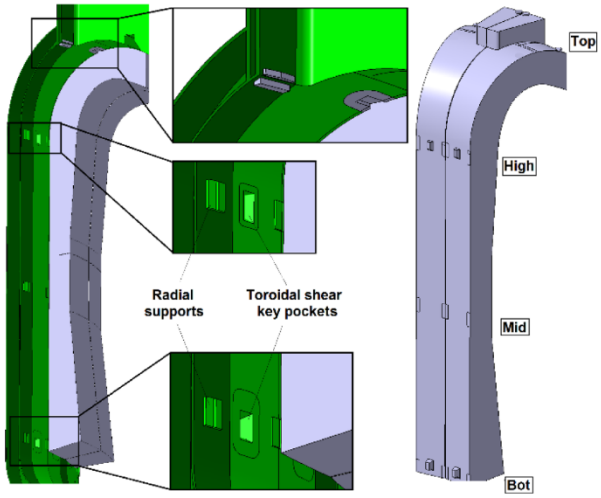

Fig. 24. Supports of the inboard BB segments in the VV-supported concept.

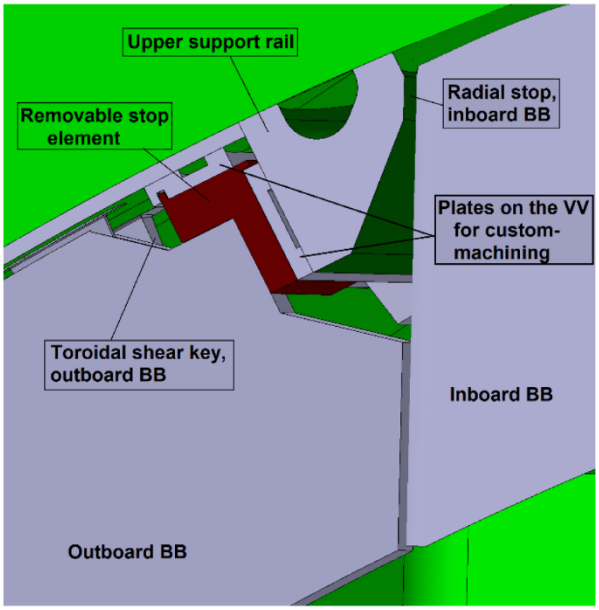

Fig. 25. Horizontal cross-section through the upper support rail including the radial stop of the inboard segments and the removable stop element (brown) at the upper supports of the outboard segments providing support in both radial directions.

8.6.4. *Radial stops - outboard segments*

The radial stops provide support to the outboard segments against forces pushing them away from the plasma. They are integrated with their vertical supports, see next paragraph.

8.6.5. *Vertical supports*

During *installation* and *in-vessel maintenance* the BB segments are at 20 °C and ~50–80 °C, respectively, see Table 5. In these states there is a gap of ~20 mm at the upper vertical supports. This gap is closed prior to plasma operation when the BB segments are heated in *standby* to ~300 °C and hence vertically supported also on the top. In case upward loads occur on the BB segments due to halo currents in upward vertical displacement events (VDEs), see paragraph 8.7.2, impact loads on the upper vertical support are therefore avoided.

At the upper vertical supports of the inboard segments a gap of ~20 mm occurs naturally during the final installation movement, which is a small vertical drop. The final installation movement of the outboard segments however is a larger vertical drop of ~120 mm [55] to engage with the bottom supports, see Fig. 26. Consequently, after installation there will be a vertical gap of at least 120 mm. The BB thermal expansion within the VV in *standby* is ~33 mm only [13]. Hence in order to fill the gap, removable stops will be inserted after the BB installation, see Fig. 25. These will be adjusted to retain a similar-size gap prior to BB heat-up as that above the inboard segments (~20 mm).

8.7. *BB segment loads*

8.7.1. *Accelerations*

In the current reference configuration the volume of the individual inboard and outboard BB segments is approximately 15m^3 and 21m^3, respectively. The corresponding mass – assuming the heavier water-cooled lead-lithium (WCLL) concept - is approximately 125 and 180 tons, respectively.

Plasma disruptions can accelerate the BB even more severely than seismic events. Seismic loads are therefore mainly relevant during machine shutdown when the toroidal field is off and the blanket support concept cannot rely on the ferromagnetic force.

8.7.2. *EM loads*

The following types of EM loads may act on the BB segments and are summarized in Table 6: (i) the magnetic field gradient causes forces on the BB ferromagnetic steel mainly in the radial direction due to the toroidal field gradient, (ii) currents induced in the BB segments as a consequence of magnetic field variations, mainly due to a toroidal field coil fast discharge (TFCFD), a plasma thermal quench or a plasma current quench (CQ), and (iii) currents from the plasma halo region flowing in the BB during VDEs.

Material irradiation results indicate a decrease of the saturation of the magnetization of up to 30% due to neutron irradiation with fluences several orders of magnitude lower than those expected in DEMO [71]. The BB support concept presented here is relatively robust against a reduction of the ferromagnetic forces since the BB is supported in both radial directions. Nonetheless, a quantification of this effect is needed to allow a complete verification of the BB support concept.

8.7.3. *Thermal conditions*

Since the BB support concept over-constrains the BB segments in some degrees of freedom temperature increases and thermal gradients of

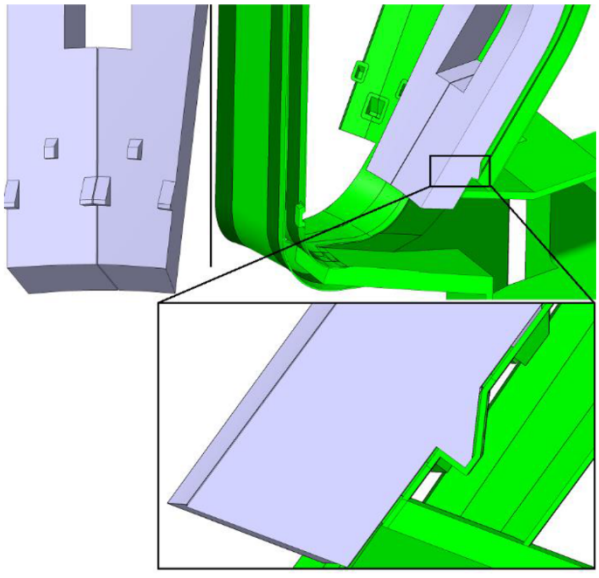

Fig. 26. Lower supports of the outboard BB segments providing support in both radial directions.

Table 6
Most notable loads acting on the inboard and outboard BB segments respectively, see also [70].

[MN, MNm]	Inb.	Outb.
F_{rad}		
- ferromagnetic	−7	−2
- TFCFD	−12	3
- fast VDE, thermal quench	7	−3
- fast VDE, current quench	±7	±2.5
F_{vert} (upward)		
- slow VDE	9	
M_{rad} (reacted on toroidal shear keys)		
- fast VDE, current quench	13	10
M_{tor} (causing radial forces)		
- fast VDE, thermal quench	9	3

the BB segment can cause significant support reaction forces. At this point only a selection of thermal conditions has been considered in the assessment of the BB supports. A complete assessment that needs to be carried out in the future will require the consideration of the detailed BB design and of transient conditions, e.g. during plasma ramp-up.

We considered (i) the approximate thermal condition of the helium-cooled pebble bed (HCPB) concept as it experiences more extreme temperature gradients in the range ~[300–500 K], [64], (ii) the temperature state during in-vessel maintenance when the radioactive decay generates heat in the passive BB [67], and (iii) the high temperature established in the BB in case of an ex-vessel loss of BB coolant during plasma operation when the maximum BB temperature occurs: initially 585 °C (in the FW) [65], and after approximately 1 h about 500 °C and 650 °C depending on the BB concept being WCLL or HCPB respectively [66].

8.8. Verifications

8.8.1. Reaction forces

The reaction forces on the BB supports of the five different BB segments were determined for different load cases and in different machine states [55]. The determined reaction forces do not exceed the design loads of the support structures, which are 4 MN for radial and vertical supports and 2 MN for toroidal supports.

I Loads during flat top and ex-VV LOCA: The vertical loads on the top and bottom supports remain well within the design limits of the support structures. This shows that both the inboard and outboard segments are sufficiently flexible.

II Loads due to TFCFD: The TFCFD generates a high compression of the blanket segments towards the VV. On the inboard segments high support reaction forces of up to ~4 MN and also high stresses in the BB structure occur. On the outboard segments the EM load due to the TFCFD may slightly exceed the ferromagnetic force. The loads on the radial stops are however well within the design limits.

III Loads during fast disruption: During both the thermal and fast current quenches, radial loads occur on some inboard and some outboard segments that exceed the ferromagnetic loads. The support condition of the inboard BB changes in this case. The inboard segment is then radially supported only on the top and on the bottom.

8.8.2. Stresses in BB segments

The stresses in the BB segments have been calculated using a finite element model [56]. The stress limit for primary membrane + bending stresses in the BB is ~240 MPa, that for primary + thermal stresses ~480 MPa [72]. The stresses in the BB segments were assessed with the aim of identifying potential major issues rather than to verify the BB structural integrity. The calculated stress level in the BB segments is shown for example during normal operation (flat top) in Fig. 27. It was also found that in an ex-vessel LOCA the yield stress of ~320 MPa at 550 °C is exceeded in some regions of the BB. The extent of any permanent plastic deformation needs to be well controlled as it could negatively affect the support condition and the FW alignment. During a fast current quench and during a TFCFD large stresses are generated in the inboard BB FW of up to ~300–350 MPa. Additional radial supports on the inboard wall and/or modifications of the BB design might be suitable mitigation strategies.

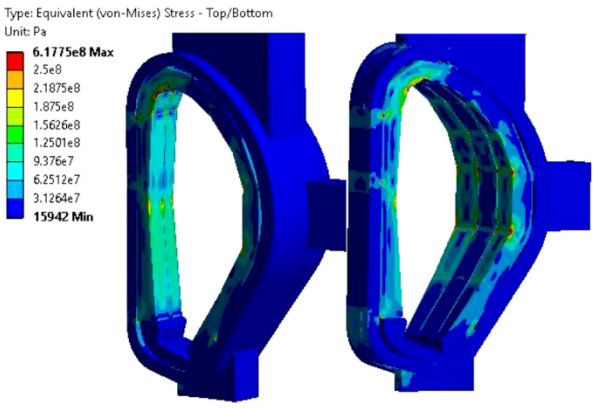

Fig. 27. Membrane + bending stress distribution in the BB segments during flat top; the orange contour is manually defined as 250 MPa.

8.8.3. BB deformation/FW alignment

The positioning tolerance of the BB FW is expected to be within ±5–10 mm, see Section 2.2. The consequent increase of FW heat loads due to charged particles was found to be not higher than ~25% and hence tolerable [73]. Additional misalignment of the FW occurs due to the thermal deformation of the BB segments during operation. While the inboard FW deforms by only few mm on the outboard side up to 16 mm are predicted. However, the presence of plasma limiters on the outboard side that protrude beyond the BB FW [5] is expected to prevent excessive heat loads on any leading edges of the BB FW.

9. Summary

In the DEMO PCD Phase the principle emphasis was on the integrated design of the major component of the tokamak. VV: This includes a design concept of the VV that is the central component of the DEMO tokamak and integrates the various in-vessel components. Its ports are configured in-between the magnetic coils and connected with metallic bellows to the cryostat. The DEMO VV is, much like the ITER VV [15], a welded double-wall structure made mainly of austenitic steel 316L (N)-IG. The inboard side is reinforced by toroidal ribs and made of a higher strength steel (XM-19) to cope with the high EM loads. The design takes into account the required manufacturing processes and the required shape precision and aims at facilitating in-service inspections. In order to reduce the amount of activation waste stemming from the VV the inner shell thickness has been reduced and EUROFER is used for some of the in-wall shielding plates.

Cryostat: Two design concepts of the cryostat were developed: an ITER-like self-supported vacuum chamber and a lighter concept, which is supported against the external pressure by the bioshield. Since it is planned to investigate in the future a transfer of the confinement function from the VV to the cryostat, the self-supported concept has been presented in this article. For the top lid with a diameter of ~40 m, it is particularly demanding to achieve a design that withstands the external pressure since the large openings required to access the VV upper ports significantly reduce the membrane stiffness of the dome-shaped structure. Radial girders between the ports were implemented and provide the required stability.

Tokamak building: The cuboid tokamak building is adjacent to the assembly hall in the south and the AMF in the north. It has two annexes on its east and west sides, the tritium building and the magnet power & diagnostic building. The internal structure is dominated by the cylindrical bioshield in its center and numerous port cells arranged with the VV ports. The levels are arranged corresponding to the machine ports and to integrate the various plant systems required to supply the tokamak and the building service. The internal division of the tokamak building by levels and sealed rooms allows the segregation of the various source terms facilitating the control of accidents.

Ports: The VV has three ports per sector. The lower port mainly integrates the torus vacuum pumps and allows access to replace the divertor. The large upper ports mainly integrate the BB service pipes and allow the vertical extraction of the large BB segments into the upper maintenance hall above the bioshield. Some upper ports also integrate plasma limiters. The equatorial ports allow the integration of plasma heating and diagnostic systems. So far only the design of the EC launcher has been developed. Four equatorial ports are foreseen for the installation and replacement of plasma limiters at the mid-plane, both inboard and outboard, as well as on the lower outboard side. Upon removal of an outboard mid-plane limiter a multipurpose deployer [43, 44] can enter into the plasma chamber to perform various tasks.

BB attachments: The mechanical integration of the BB segments into the VV is a prerequisite for the choice of the vertical BB segment architecture, see also [74]. The BB support concept does not require fasteners or electrical straps connected to the VV and therefore significantly reduces the complexity of the BB remote replacement. Each BB segment is individually supported by the VV without any physical contact to other in-vessel components. It relies instead on vertical pre-compression inside the VV due to obstructed thermal expansion and radial pre-compression due to the ferromagnetic force acting on the BB structure in the toroidal magnetic field. Preliminary verifications are promising but further developments and validations by analysis and testing are required.

Author statements

C. Bachmann: Conceptualization, methodology, validation, supervision, original draft
L. Ciupinski: Formal analysis, review and editing
C. Gliss: Conceptualization, review and editing, visualization
T. Franke: Conceptualization, review and editing
T. Härtl: Conceptualization, review and editing
P. Marek: Formal analysis, review and editing, visualization
F. Maviglia: Conceptualization, review and editing
R. Mozzillo: Conceptualization, review and editing, visualization
R. Pielmeier: Formal analysis, conceptualization
T. Schiller: Conceptualization
P. Späh: Conceptualization, review and editing, visualization
T. Steinbacher: Conceptualization, visualization
M. Stetka: Conceptualization, review and editing, visualization
T. Todd: Review and editing
C. Vorpahl: Conceptualization, review and editing, visualization

Declaration of Competing Interest

The authors declare that they have no known competing financial interests or personal relationships that could have appeared to influence the work reported in this paper.

Acknowledgments

This work has been carried out within the framework of the EUROfusion Consortium and has received funding from the Euratom research and training program 2014–2018 and 2019–2020 under grant agreement No 633053. The views and opinions expressed herein do not necessarily reflect those of the European Commission.

References

[1] Antonius Johannes Donné, Roadmap Towards Fusion Electricity, J. Fusion Energy 38 (5) (2019) 503–505.
[2] G. Federici, et al., The EU DEMO Staged Design Approach in the Pre-Concept Design Phase, 2021 this edition.
[3] G. Federici, et al., Overview of the DEMO staged design approach in Europe, Nucl. Fusion 59 (6) (2019), 066013.
[4] Neill Taylor, Pierre Cortes, Lessons learnt from ITER safety & licensing for DEMO and future nuclear fusion facilities, Fusion Eng. Des. 89 (9–10) (2014) 1995–2000.
[5] F. Maviglia, et al., Impact of Plasma Thermal Transients on the Design of the EU DEMO, in: 14th International Symposium on Fusion Nuclear Technology (ISFNT-14), 2019.
[6] Ch Bachmann, et al., Issues and strategies for DEMO in-vessel component integration, Fusion Eng. Des. 112 (2016) 527–534.
[7] D. Flammini, et al., Neutronics studies for the design of the European DEMO vacuum vessel, Fus. Eng. Des. (2016) 784–788.
[8] Ch Bachmann, et al., Overview over DEMO design integration challenges and their impact on component design concepts, Fusion Eng. Des. 136 (2018) 87–95.
[9] Bharat Doshi, et al., Design and manufacture of the ITER cryostat, in: 2013 IEEE 25th Symposium on Fusion Engineering (SOFE), IEEE, 2013.
[10] Anil K. Bhardwaj, et al., Overview and status of ITER Cryostat manufacturing, Fusion Eng. Des. 109 (2016) 1351–1355.
[11] Łukasz Ciupiński, et al., Design and Verification of a Non-Self-Supported Cryostat For DEMO Tokamak, Division of Materials Design, 2019.
[12] G. Federici, et al., Magnetic Confinement Fusion—Technology—Fusion Core. Reference Module in Earth Systems and Environmental Sciences, 2021, https://doi.org/10.1016/B978-0-12-819725-7.00050-7.
[13] Thomas Haertl, et al., Rationale for the selection of the operating temperature of the DEMO vacuum vessel, Fusion Eng. Des. 146 (2019) 1096–1099.
[14] K. Ioki, et al., ITER vacuum vessel design and construction, Fusion Eng. Des. 85 (7-9) (2010) 1307–1313.
[15] C.H. Choi, et al., Status of the ITER vacuum vessel construction, Fusion Eng. Des. 89 (7-8) (2014) 1859–1863.
[16] B.C. Kim, et al., Fabrication of the KSTAR vacuum vessel and ports, Fusion Eng. Des. 83 (4) (2008) 573–579.
[17] A. Cardella, et al., Construction of the vacuum vessels and the magnet supporting structures of Wendelstein 7-X, Fusion Eng. Des. 82 (15–24) (2007) 1911–1916.
[18] A.S. Pokrovsky, S.A. Fabritsiev, Effect of neutron irradiation on tensile properties of austenitic steel XM-19 for the ITER application, J. Nucl. Mater. 417 (1–3) (2011) 874–877.
[19] Mark R. Gilbert, et al., Waste implications from minor impurities in European DEMO materials, Nucl. Fusion 59 (7) (2019), 076015.
[20] A.-.A.F. Tavassoli, et al., Materials design data for reduced activation martensitic steel type EUROFER, J. Nucl. Mater. 329 (2004) 257–262.
[21] AC07743168, Anonymus, Integrity of Reactor Pressure Vessels in Nuclear Power plants: Assessment of Irradiation Embrittlement Effects in Reactor Pressure Vessel Steels, Internat. Atomic Energy Agency, 2009.
[22] Kembleton, Richard, et al., "Design Space Exploration and design choices under consideration", this edition. 2021.
[23] J.-.M. Martinez, et al., Structural analysis of the ITER vacuum vessel regarding 2012 ITER project-level loads, Fusion Eng. Des. 89 (7–8) (2014) 1836–1842.
[24] Rocco Mozzillo, Christian Bachmann, Giuseppe Di Gironimo, Structural assessment on DEMO lower port structure, Fusion Eng. Des. 121 (2017) 348–355.
[25] Curt Gliss, et al., Initial integration concept of the DEMO lower horizontal port, Fusion Eng. Des. 146 (2019) 2667–2670.
[26] Christian Bachmann, et al., Initial definition of structural load conditions in DEMO, Fusion Eng. Des. 124 (2017) 633–637.
[27] D. Combescure, et al., Structural analysis and optimization of the ITER-Tokamak complex, in: First Kashiwasaki International Symposium on Seismic Safety of Nuclear Installation. Workshop 2-Seismic Isolation of Nuclear Facilities, 2011.
[28] Domen Kotnik, et al., Assessment of sky-shine in DEMO during breeding blanket maintenance, Fusion Eng. Des. 167 (2021), 112348.
[29] Aljaž Čufar, et al., Shielding concept and neutronic assessment of the DEMO lower remote handling and pumping ports, Fusion Eng. Des. 157 (2020), 111615.
[30] C. Gliss, et al., Integration of DEMO radioactive fluids piping into the tokamak building, submitted to *Fusion Engineering and Design*Mozzillo, Rocco, et al. "Integration of LiPb loops for WCLL BB of European DEMO, Fusion Eng. Des. 167 (2021), 112379.
[31] Thomas Franke, et al., The EU DEMO equatorial outboard limiter — Design and port integration concept, Fus. Eng. Des. 158 (2020), 111647.
[32] Pavel Pereslavtsev, et al., DEMO tritium breeding performances with different in-vessel components configurations, Fusion Eng. Des. 166 (2021), 112319.
[33] Christian Vorpahl, et al., Initial configuration studies of the upper vertical port of the European DEMO, Fusion Eng. Des. 146 (2019) 2469–2473.
[34] Gianfranco Federici, et al., DEMO design activity in Europe: progress and updates, Fusion Eng. Des. 136 (2018) 729–741.
[35] Oliver Crofts, et al., Overview of progress on the European DEMO remote maintenance strategy, Fusion Eng. Des. 109 (2016) 1392–1398.
[36] Keelan Keogh, et al., Laser cutting and welding tools for use in-bore on EU-DEMO service pipes, Fusion Eng. Des. 136 (2018) 461–466.
[37] Stuart Budden, et al., Rescue and recovery studies for the DEMO blanket transporter, Fusion Eng. Des. 146 (2019) 2494–2497.

[38] Rocco Mozzillo, et al., Vacuum vessel Upper Port design assessment of the European DEMO, Fusion Eng. Des. 138 (2019) 10–15.
[39] Rocco Mozzillo, et al., European DEMO fusion reactor: design and integration of the breeding blanket feeding pipes" submitted to *Journal of pressure vessel and piping design*You, Jeong-Ha, "Limiters for DEMO wall protection: initial design concepts & technology options", this edition (2021).
[40] Maviglia, Francesco, et al., "Integrated design strategy for EU-DEMO first wall protection from plasma transients", this edition. 2021.
[41] A. Loving, et al., Pre-conceptual design assessment of DEMO remote maintenance, Fusion Eng. Des. 89 (9–10) (2014) 2246–2250.
[42] Chang-Hwan Choi, et al., Multi-purpose deployer for ITER in-vessel maintenance, Fusion Eng. Des. 98 (2015) 1448–1452.
[43] Avelino Mas Sánchez, et al., Design and Numerical Analyses of the M4 Steering Mirrors for the ITER Electron Cyclotron Heating Upper Launcher, IEEE Trans. Plasma Sci. 47 (12) (2019) 5271–5276.
[44] Siccinio, Mattia, et al., "Development of a reliable plasma-operating scenario including supporting systems (e.g. heating and current drive (HCD) and plasma diagnostics/control systems)", this edition. 2021.
[45] Thomas Franke, et al., Integration concept of an Electron Cyclotron System in DEMO, Fusion Eng. Des. 168 (2021), 112653.
[46] Tran, Minh Quang, et al., "Heating & Current Drive systems", this edition. 2021.
[47] Peter Spaeh, et al., Structural pre-conceptual design studies for an EU DEMO equatorial EC port plug and its port integration, Fusion Eng. Des. 161 (2020), 111885.
[48] Dirk Strauss, et al., Nearing final design of the ITER EC H&CD Upper Launcher, Fusion Eng. Des. 146 (2019) 23–26.
[49] M. Henderson, et al., The targeted heating and current drive applications for the ITER electron cyclotron system, Phys Plasmas 22 (2) (2015), 021808.
[50] F. Farfaletti-Casali, et al., The interaction of systems integration, assembly, disassembly and maintenance in developing the INTOR-NET mechanical configuration, Nucl. Eng. Design. Fusion 1 (2) (1984) 115–125.
[51] Max Chazalon, et al., Next European Torus assembly and maintenance, Fusion Technol. 14 (1) (1988) 156–164.
[52] D. Maisonnier, et al., Power plant conceptual studies in Europe, Nucl. Fusion 47 (11) (2007) 1524.
[53] C. Bachmann, et al., Mechanical support concept of the DEMO breeding blanket, *Fusion Engineering and Design* (submitted) (2021).
[54] Z. Vizvary, et al., Status of the DEMO blanket attachment system and remaining challenges, Fusion Eng. Des. 151 (2020), 111357.
[55] Ivan Alessio Maione, et al., Electromagnetic analysis activities in support of the Breeding Blanket during the DEMO Pre-Conceptual Design Phase: methodology and main results, Fusion Eng. Des. 166 (2021), 112285.
[56] F. Maviglia, et al., Effect of engineering constraints on charged particle wall heat loads in DEMO, Fusion Eng. Des. 124 (2017) 385–390.
[57] A.R. Raffray, et al., The ITER blanket system design challenge, Nucl. Fusion 54 (3) (2014), 033004.
[58] A. Del Nevo, et al., WCLL breeding blanket design and integration for DEMO 2015: status and perspectives, Fusion Eng. Des. 124 (2017) 682–686.
[59] Francisco A. Hernandez, et al., An enhanced, near-term HCPB design as driver blanket for the EU DEMO, Fusion Eng. Des. 146 (2019) 1186–1191.
[60] G. Mazzone, P. Frosi, Study of dynamic amplification factor of DEMO blanket caused by a gap at the supporting key, Fusion Eng. Des. 98–99 (2015) 1299–1304.
[61] S. Khomyakov, et al., Dynamic amplification of reaction forces in the blanket module attachment during plasma disruption of ITER, Fusion Eng. Des. 81 (1-7) (2006) 485–490.
[62] J. Aubert, et al., Fus. Eng. Des. 98–99 (2015) 1206–1210.
[63] G. Zhou, et al., Fus. Eng. Des. 136 (2018) 34–41.
[64] M. Draksler, et al., Analysis of the Natural Circulation of Air Inside the Vented DEMO Vacuum Vessel After an Ex-Vessel Loss of Coolant accident, Submitted to *Fusion engineering and Design*, 2021.
[65] M. Draksler, et al., Assessment of Residual Heat Removal from Activated Breeding Blanket Segment During Remote Handling in DEMO" Submitted to *Fusion engineering and Design*, 2021.
[66] J. Reich, et al., Three dimensional tolerance investigations on assembly of ITER vacuum vessel, in: 2009 23rd IEEE/NPSS Symposium on Fusion Engineering, IEEE, 2009.
[67] Sam Davis, et al., JT-60SA magnet system status, IEEE Trans. Appl. Supercond. 28 (3) (2017) 1–7.
[68] I. Maione, EM analysis of WCLL Breeding Blanket for the DEMO configuration of 2015, EUROfusion report 2018: EFDA_D_2NPNWM.
[69] Rodolfo A. Kempf, et al., Correlation between radiation damage and magnetic properties in reactor vessel steels, J. Nucl. Mater. 445 (1–3) (2014) 57–62.
[70] G. Aiello, et al., Assessment of design limits and criteria requirements for Eurofer structures in TBM components, J. Nucl. Mater. 414 (1) (2011) 53–68.
[71] Z. Vizvary, et al., DEMO First Wall misalignment study, Fusion Eng. Des. 146 (2019) 2577–2580.
[72] Chauvin, D. et al., "KDII#4 Vertical segment architecture", this edition. 2021.